

RICULTURE ROOM

CREEP OF SMALL WOOD BEAMS UNDER CONSTANT BENDING LOAD

September 1959

No. 2150



FOREST PRODUCTS LABORATORY
MADISON 5, WISCONSIN

UNITED STATES DEPARTMENT OF AGRICULTURE
FOREST SERVICE

In Cooperation with the University of Wisconsin

CREEP OF SMALL WOOD BEAMS
UNDER CONSTANT BENDING LOAD¹

By

WILLIAM S. CLOUSER, Engineer

Forest Products Laboratory,² Forest Service
U. S. Department of Agriculture

Summary

An analysis of creep occurring in small Douglas-fir beams tested at midspan under concentrated loads ranging from 60 to 95 percent of ultimate is presented. The experiments were performed under conditions of constant temperature and relative humidity that maintained the specimens at 6 or 12 percent equilibrium moisture content for periods as long as 10 years. A power law equation, $\epsilon = \epsilon_0 + at^m$, is used to describe the creep curve up to the point of inflection. Results are presented in terms of stress level, power law equation constants, creep rate, and time.

Introduction

A series of experiments was begun at the Forest Products Laboratory in 1943 to determine the behavior of small, clear, simply supported Douglas-fir beams in controlled atmospheres under three types of load applied at midspan.

The types of loading employed were: (1) Constant dead loads of predetermined size applied until failure of the beam occurred; (2) loads applied by dropping shot into a box hung from the beam at a constant rate so as to cause failure in a predetermined time; and (3) repeated load cycles to failure in which the beams were alternately subjected to dead loads for a week and then allowed to recover for a week after removal of the loads.

In this report are presented the results obtained in series of tests performed with constant loads applied until failure of the specimen took place. The behavior of the specimens is analyzed with respect to such factors as amount of deflection, rate of deflection, and life of the specimen for different atmospheric conditions.

The increasing deflection of a loaded beam with the passage of time is commonly called creep. Under proper conditions, creep is common to all materials, and it has long been recognized as an important consideration in the design of timber structures that must have a long life, often under heavy

¹This report is based upon a thesis for a Ph.D. degree in mechanics at the University of Wisconsin.

²Maintained at Madison, Wis., in cooperation with the University of Wisconsin.

loads. The results of creep may be observed in buildings in the form of sagging joists and rafters or the more familiar example of sagging bookcases and storage shelves.

Surprisingly little work has been done on this problem up to the present, the bulk of it in recent times. The decrease in breaking strength of a timber beam under a continuing load has been recognized at least since the beginning of the eighteenth century (44).¹ Buffon (8) experimented with oak beams in 1740 to determine a safe load for long-time loading. Tiemann (59) reported that Herman Haupt made a series of tests to show the effect of prolonged loading on various woods in 1841, and that Denton and Riesenberger tested long-leaf pine in bending in 1880. Other work, minor in scope, was also done.

Most of the work in the field of creep, however, has been done during the present century, possibly because of the emphasis on research during the past two major wars and the diminution of natural resources in the more highly developed parts of the world. A number of investigations have been carried out, starting with Tiemann's work at Yale in 1907-09 (58). Some work was done in Germany in the 1930's. Vorreiter (60) summarized the work of K. Egner in 1934 on "pine," which included some loading periods as long as 700 days. Kollman (29) concisely related the work of Ph. Roth in 1935 and the well-known work of O. Graf (23). In this country, Draffin and Muhlenbruch ran bending tests on balsa with durations from 100 to 600 days (14).

In 1947, L. W. Wood reported on the first results of the Forest Products Laboratory experiments (63). In Australia, Kingston and Armstrong (27,28) reported work on initially green Tasmanian oak beams, which was followed in 1953 by Armstrong's work with 12 small air-dried specimens (5). From 1956 to 1958 Hideo Sugiyama of Meiji University, Tokyo, completed a series of tests on small beams of Japanese woods, most of which were for 3 months or less, but some of which extended to approximately a year (54,55).

In all of the work reported, there was little if any control of atmospheric conditions. The difficulties involved in maintaining a closely controlled atmosphere are many, especially when this must be done for very long periods of time. The work which comes closest to attaining this goal is the series of tests at Madison.

Details of these various experiments are to be found in the references cited. The tests indicated rough agreement on the following points:

(1) A load less than 45 to 60 percent of the short-time ultimate load (based on the modulus of rupture) did not cause failure in the beams during the time allotted to the experiments.

¹Underlined numbers in parantheses refer to literature cited at the end of this report.

(2) An increase in moisture content during the test caused an increase in the deflection of the beam although the load remained constant.

(3) The higher the moisture content of the wood at the start of the test, the greater was the total deflection at any given time.

The results of these tests, together with long experience in the behavior of structural timber, are reflected in the recommendations made for long-time loading design stresses by various organizations.

The Forest Products Laboratory (20) recommends the use of a basic working stress suitable for use in long-time loading under full load. A factor of nine-sixteenths is used to convert the ultimate strength in the standard short-time test to a corresponding strength under long-time loading. Other factors are then applied to arrive at the basic stress. This long-time stress value is then modified for short times, for example 10 years, by factors obtained from an empirical curve derived by Wood (64).

In the "National Design Specifications for Stress-Grade Lumber and Its Fastenings" (40), a "normal loading" presumed safe for a cumulative 10-year duration of load is used as a base. This figure can then be adjusted to fit the duration expected.

The problem of the large deflection (which may be more than twice the initial deflection without failure) is simply solved by halving the modulus of elasticity in static bending or by setting the initial allowable deflection at one-half the long-time allowable deflection (20).

Creep

As is well known, the static testing of materials is often not sufficient for the determination of their behavior for present-day applications. The rate of application of the load and the time that the load remains in place are extremely important factors. Consideration of these factors requires that information be obtained about behavior with respect to time as well as data on short-time stresses and strains.

The responses of nearly all materials to loads of long duration are similar, although from the standpoint of mechanism the similarity may be more apparent than real.

If deformation (expressed as strain, elongation, or deflection) is plotted against time, a curve similar to that shown in figure 1 will result. The curve can be divided into four parts. The initial deformation, OA, is that occurring when the load is applied. It is, for all practical purposes, usually considered to be instantaneous and, depending upon the magnitude of the load, may be composed of elastic, delayed elastic, and plastic

deformations. These, however, are developed in a relatively short time as the load increases and are therefore considered together for constant load tests.

The primary stage, AB, of the creep curve, also called the transient creep stage, describes a period during which the rate of deformation constantly decreases. This decrease continues until the secondary stage, BC, is attained. The secondary stage, or steady-state part of creep, is usually considered the period of constant rate of deformation. Thus, BC is a straight line of minimum slope. This region is joined smoothly to a tertiary stage, CD, in which the deformation rate increases and failure of the specimen ultimately occurs.

In practice, the form of the curve may depart widely from that shown in figure 1. Figure 2 shows the forms usually taken as either the load or the temperature is raised. The curves from A to D represent increasing temperature or increasing load.

The slope of the curve may be dependent upon other factors, such as moisture content of the specimen, changing ambient conditions, and structural changes in the specimen. This is especially true in hydrophilic substances, such as concrete, many plastics, and wood. Structural changes are important in metals and in the aging of concrete and plastics. Rotherham (47) shows a few of the infinite variations that can occur in practice to influence the shape of the curve.

The steady-state region, BC, has been the subject of much study in the search for relations that would permit prediction of the time of failure of a given specimen from the results of short-time tests. Although the region is most often treated as a straight line, a question arises as to whether it is not actually a very flat reverse curve with a point of inflection, such as the more pronounced example D in figure 2, with a point of inflection E. The problem here is that the measurement of such small deformations is either impossible with the gages at hand, or the magnitude of other factors in the experimental setup effectively masks the small changes in deformation. The straight-line part often shrinks to a point as the temperature and load are increased.

At low temperatures and low loads, the creep rate may appear to become zero. Although this is a value often cited in the literature as a limiting rate, it has not been shown that failure will not occur, merely that failure has not occurred. The limiting creep stress is a useful idea from an engineering viewpoint, however, since a material which has a zero (or near zero) creep rate for "a very long time" can be extremely valuable.

The final portion of the curve shown in figure 1 has been investigated far less than have the other parts. Since a material which has entered this stage has, for design purposes, failed, many tests are stopped when this stage is reached in order to save time and money. A further deterrent with metals has been the belief that failure in this stage was due to necking of

the specimen. This belief arose as a result of the early work of Andrade (4) and others, who maintained that this stage was absent under constant stress loadings. From the experiments of Sully and others (57), the existence of this final stage in metals under constant stress is now recognized.

Creep of Metals

Extensive study has been given to determining the effect of external and metallurgical factors upon creep of metals and the mathematical expressions that relate the observed creep variables. Creep is basically affected by the applied stress, the composition of the specimen, and the size and number of the crystals in the specimen.

Primary creep in metals is due largely to slip. The amount of slip depends upon the stress and the temperature, and the slip rate decreases with time. Secondary creep is attributed primarily to grain boundary movements. The sliding of the grain boundaries allows a substantial amount of deformation, which can be interpreted as viscous flow and treated as a rate process. The third stage is one of progressive internal fracture that develops directly from the grain boundary deformations of the second stage.

Any or all of these processes (together with others not mentioned) may be simultaneous. In addition, the temperatures at which creep usually is important in metals may induce significant changes in the structure and properties of the metal, which can complicate the creep processes.

Comprehensive treatment of the creep of metals may be found in references (1), (10), (41), (47), (51), and (56).

Creep of Concrete

Concrete is an intimate mixture of a hardened water-cement paste and a coarse material of varying composition and particle size, called the aggregate. Under long-time loading, concrete undergoes creep deformation, which increases at a decreasing rate while the load is acting. The heterogeneous nature of concrete and the colloidal nature of the cement paste allow many deformation processes to occur during long-time loading, such as viscous flow of the water-cement paste, plastic flow in the crystalline aggregate, closure of voids, and flow of water from the cement gel and the capillaries in the mass as a result of external loads and drying. The changes in water content just mentioned depend not only upon the relative humidity of the external atmosphere but also upon the moisture gradient within the capillaries. The amount of deformation that can be ascribed to each process is variable because of the many concrete mixtures that are made possible by changing the composition or the proportions of the ingredients.

Since some of the deformation processes are dependent on time, such factors as age before loading, treatment during aging and curing, the magnitude of the load, and the length of time that the load is applied contribute as much to the creep of concrete as the materials used in making it.

Some surveys of the creep of concrete give extensive bibliographies (19), (31), (42), and (61).

Creep of Wood

Wood is a complex, anisotropic, porous, naturally expanded material. The composition varies slightly from species to species, but the most important constituents common to all are cellulose, hemicellulose, and lignin. Cellulose and hemicellulose make up 70 to 80 percent of the weight of oven-dry wood, and lignin 20 to 30 percent.

The cellulose molecule has hydroxyl (-OH) groups at regular intervals. These are responsible for the adsorption of water molecules and for bonding cellulose molecules to each other in the crystallites that form the minute structure of the cell wall. Although the resulting individual bonds are weak, there are so many that the total binding energy is great enough to prevent the separation of the cellulose chains by water. This force also prevents the melting of cellulose at high temperatures.

This exclusion of water from the interior of the crystallite leads to the adsorption of water only in the amorphous regions and on the surfaces of the crystallites. In a humid atmosphere dry wood adsorbs moisture, the water molecules becoming attached to the accessible hydroxyl groups. The attachment produces swelling of the wood, principally in the radial and tangential directions and to only a slight extent longitudinally, since the fibrils are approximately parallel to the axis of the cell. This suggests for wood the same possibility that has been presented for concrete (45,46), that unequal shrinkage stresses may contribute to creep.

The presence of water facilitates plastic strain in wood by weakening bonds between some of the cellulose chains. An increase in temperature will weaken the bonds by increasing thermal molecular movement.

If applied strains are not large enough to break bonds, the wood will behave elastically. If the strains do break bonds, there will be differential movement between the chains with exchange of bonds and inelastic strain. Permanent strain can also occur upon rupture of molecules or by shearing of the crystallites. These processes would be more likely to occur in the final stages of creep or at a very high creep rate.

In the light of the structure and chemistry of wood, these assumptions about creep mechanisms are valid. It must be remembered, however, that wood is a natural product and, as such, has a host of growth features such as knots, pitch pockets, and grain irregularities, that introduce an empirical factor into the description of the creep process.

Excellent summaries exist on high polymers and their properties (18, 43, 49). The structure of wood and cellulose and the changes occurring with moisture changes are to be found in (6, 29, 38).

The Mathematical Description of Creep

Mathematical expressions to describe creep range from simple relationships that fit experimental data to complex relationships based on assumptions regarding the creep mechanism.

In the following discussion, a few of the more widely used treatments are outlined. The chief variables involved are either creep and time, or creep, stress, and time.

The fact that the creep curve is apparently linear in the secondary stage led McVetty (35) to formulate an expression as follows:

Assume an asymptotic approach to the minimum creep rate (the slope of the portion BC in figure 1); then

$$\frac{d\epsilon}{dt} - V_0 = Be^{-Kt}$$

where $\frac{d\epsilon}{dt}$ is the rate of change of deformation, V_0 is the minimum creep rate (slope of BC), B and K are constants, and t is time.

Integrating

$$\epsilon = \epsilon_0 + V_0 t - \frac{B}{K} e^{-Kt}$$

where ϵ is the total deformation and ϵ_0 the intercept of the straightline part, on the deformation axis.

For large t , this approaches the expression:

$$\epsilon = \epsilon_0 + V_0 t$$

This equation has been extremely useful in the study of primary and secondary creep. Of course, it is of no value beyond the straightline range and is not accurate for the many materials that have no straightline part to their creep curve. It is still used and forms the basis for many extremely complicated expressions (36).

Weaver (62) assumed that the creep rate is inversely related to time and approaches a constant value.

$$\frac{d\epsilon}{dt} = V_0 + \frac{a}{t}$$

where a is a constant and the others as before. Then

$$\epsilon = V_0 t + a \cdot \log t + \text{a constant}$$

For metals, these terms are interpreted as structural changes that modify viscous flow.

The fact that many materials yield a straight line when the logarithm of creep is plotted against that of time has often been noted. The expression obtained from this line is the power law. This empirical treatment is attributed to Sturm, Dumont, and Howell (53), although Filon and Jessop utilized this relation in 1923 (15). The plot leads to an equation:

$$\log (\epsilon - \epsilon_0) = \log b + m \log t$$

where ϵ is total creep, ϵ_0 is a constant derived from the data which includes elastic and plastic deformation, and b and m are constants.

This gives

$$\epsilon = \epsilon_0 + bt^m$$

This expression has been used to describe creep behavior in metals, plastics (11,12,15,16,17,49), and crystalline nonmetals (1).

In the field of concrete, similar empirical expressions have been employed. For example, Straub (52) used a generalized power law containing as variables stress, deformation, and time.

$$\epsilon = k\sigma^p t^q$$

where ϵ is the unit plastic deformation after time t , k a coefficient obtained from tests, σ the unit stress, and p and q are constants depending upon the elastic properties at the beginning of the stressed condition.

Shank (50) proposed a modification based on the assumption that creep is proportional to the unit stress.

$$y = Ct^{1/a}$$

where y is the plastic flow per unit stress, t is time, and C and a are constants determined for the particular concrete and the loading conditions.

Lorman (33) used a hyperbolic form based on the work of Ross:

$$\epsilon = \frac{m t}{n + t} \sigma$$

where ϵ is creep strain, m a constant called the "creep coefficient," n a creep-time constant, t is time reckoned from when the load is applied, σ is stress, and m and n are constants determined from the conditions of loading.

McHenry (34) related creep, time, and loading and aging factors in an expression for the creep due to a unit load.

$$Q = \alpha(1 - e^{-rt}) + \beta e^{-pk} (1 - e^{-mt})$$

where Q is creep strain due to unit load, α , β , r , p , and m are constants evaluated from the experimental conditions, and k is age at time of loading. This equation is based on the superposition principle of Boltzmann (7). Leaderman (32) and Gross (24) have given extensive treatments of this principle, which has had wide application in the primary creep of visco-elastic materials. Small strains, deformations which are linear functions of the load, and complete recovery of creep are basic assumptions in this theory, which states that the total deformation of a material with a history of varying loads (removal of a load being considered a negative application of the same load) is the sum of the deformations that would be produced from each of the loads applied separately.

Several other representations that are appearing in the literature should be mentioned. Although certain of them are claimed to have a basis in the fundamental relations of the physics and chemistry of matter, the work involving them is as yet on a semiempirical basis and much remains to be done before any of them can be considered as nonempirical.

Nadai and McVetty (39) employed the empirical relation:

$$V = V_0 \sinh \left(\frac{\sigma}{\sigma_0} \right)$$

where V is the minimum creep rate, σ is the applied stress, and V_0 and σ_0 are experimentally determined constants with dimensions of strain rate and stress respectively. Although the occurrence of a hyperbolic sine function in rate theory (21) has been considered to be an additional support for the Nadai expression, Nadai apparently developed the relation originally as an empirically better fit than the power law.

The rate process theory was originally applied to chemical reactions and to the flow of liquids. It was extended to the case of solids by Kauzmann (26) and many others, until a large literature now exists. Very briefly, the overall process is the sum of numerous unit processes or units of flow. These units may be molecules for simple fluids, subgrains or dislocations for metals, and portions of chains in linear polymers. The units are assumed

to be in thermal equilibrium and may only be moved to an adjacent position by a shear force. This is accomplished by providing sufficient external force to overcome the potential energy barriers that keep the units in statistical equilibrium. This, in turn, is assumed to be effected by lowering the potential in the direction of action and raising it in the opposing direction. The minimum energy supplied for movement is called the activation energy. Perhaps the chief objections to the theory are the numerous parameters to be determined and the fact that it is applied principally to secondary stage creep. Nevertheless, the activation energy approach does attempt to tie together parameters obtainable from other types of experiments than creep.

Recently some "parameter" methods have been developed from the rate theory background in attempts to predict long-time strength from short-time tests. They all consist of some relation between the parameters of time or rate and temperature and various experimentally determined constants. Two of the simpler expressions are mentioned here:

Perhaps the simplest is the Larson-Miller parameter (30) based on an equation developed by Holloman and Jaffe for the tempering of steel:

$$K = T(C + \log t)$$

where C is a constant, T is the absolute temperature, and t is the time to rupture. C is usually taken as 20, but this is not necessarily a good practice, since 20 is an average for many metallic alloys. The parameter has been used for some work in plastics (22).

The Manson and Haferd parameter (37) is based on experimental work rather than rate theory. It is of the form:

$$K = \frac{T - T_a}{\log t - \log t_a}$$

where T_a and t_a are temperature and time constants taken from constant stress tests at fairly short time.

In use, the logarithm of the initial stress is plotted against the parameter K for rupture times at high temperatures and extrapolated to lower temperatures.

A comparison of the various parameters dealing with metals is to be found in reference (25). Reference (9) has a comparison of several parameters used on glass-reinforced plastic laminates, with carefully worked examples. The proposed "Tentative Tests for Conducting Creep and Time-for-Rupture Tension Tests of Materials" of the American Society for Testing Materials (2) states in section 11 that these parameter methods must be employed with caution until more data are obtained.

Method of Test

The plan of the tests to be described was organized by G. W. Foster of the Forest Products Laboratory in 1945. L. W. Wood, also of the Laboratory, modified the plan slightly and started the test series. The scope of this test program is indicated in the Introduction. The following description is limited to the experiments involving beams loaded to failure by constant load.

The beams to be tested were 1 by 1 by 22 inches in size and were cut from flat-sawn, straight-grained, Douglas-fir planks 3 inches thick by 7 to 9 inches wide selected from Laboratory stock. Each bending-test specimen was flanked by two ring-matched control specimens. Figure 3 shows a few of the planks. The locations of the beams within the planks are marked by the pencilled squares on the ends of the pieces.

Table 1 shows the numbers of creep specimens and controls tested. From some planks, five specimens were cut, the middle beam being used as a control for both creep specimens.

Beams were brought to equilibrium with, and tested in, three atmospheric environments: 75° F. and 64 percent relative humidity, 80° F. and 65 percent relative humidity, and 80° F. and 30 percent relative humidity. In the first two, wood comes to an equilibrium moisture content of approximately 12 percent, and in the last, approximately 6 percent.

During the tests, the specimens were loaded on a tangential face; that is, with the growth rings horizontal. Forty-eight controls were loaded at a testing machine head speed of 0.084 inch per minute. One hundred seventy-five were tested at a constant loading rate of 1 pound per second by dropping lead shot through a calibrated orifice into a box suspended at the mid-point of the specimen.

A deflection rate at the center of the beam of 0.084 inch per minute over an 18-inch span is equivalent to the 0.10 inch per minute specified in ASTM Specification D 143-52 (3). This is based on an outer fiber strain rate of 0.0015 inch per inch per minute. The 1-pound-per-second loading rate gives a slightly lower strain rate, but within the 25 percent allowed. The 75-pound-per-minute rate is nearly equivalent to the standard rate.

The moduli of rupture were computed for the controls, and the average modulus of rupture of the two controls for each creep specimen was assumed to be the modulus of rupture of the creep specimen. The load corresponding to a pre-determined percentage of this average modulus of rupture was computed and then applied to the creep specimen.

Figure 4 shows four beams under test. The load was hung from the center of each beam by means of an iron stirrup that terminated at its lower end in a wood platform upon which steel or lead bars and lead shot bags were placed.

The bars and bags were gently applied at an approximate rate of 75 pounds per minute. Care was taken to minimize impact loading caused by too rapid application of the weights. The loads placed on the beams were approximately equal to the calculated load, but no attempt was made to equal the calculated loads precisely. The load levels in table 1 are therefore purely nominal. A few of the higher level loads were applied with the apparatus used to load the controls. A protective framework was placed around each test stand to prevent accidental jarring of the creep specimens.

The beams were simply supported on knife edges and rollers on 18-inch centers, and deflections were measured with a dial indicator reading to 0.001 inch. The bar supporting the dial indicator and the strap at the center of the beam were pinned with small brads at the neutral axis. The dial indicator was attached to the center strap with fine wire and lightly preloaded, so that all possible play was eliminated from the indicator linkages.

The control test data consisted of load and deflection measurements from the start of loading to failure, together with observations on the behavior of the specimen.

Deflection at the center and the time of reading comprised the bulk of the creep-test data. Careful records were taken of changes in the conditioning of the rooms in which the specimens were kept, and the behavior of the beams was closely watched. Observations were taken at intervals of a minute or less during loading and at less frequent intervals as the deflection rate decreased with time. For the more extended tests (lower load levels), readings were taken once a day or even once a week.

An attempt was made at all times to record the progress of the failure of the beams. For short-time tests at high loads no problems were encountered, but the failure of the beams tested with small loads was more difficult to predict. Consequently, times recorded for failures that occurred on the weekend or at night could be somewhat in error. If a failure was expected, an automatic recorder was employed that consisted of a rubber tube connected to a clockwork-driven pressure recorder. When a beam failed, the platform holding the weight dropped on the tube and compressed it. The resulting increase in pressure was recorded on the chart.

Mathematical Treatment of Data

The experimental data for the constant load series of tests consisted of load-deflection data for the controls, the load, and the deflection-time data for the test specimens, together with the record of the ambient conditions during the tests. The time of failure was obtained directly with an automatic recorder or, in the case of unexpected failure, could be estimated reasonably well.

The average of the moduli of rupture of the two controls for each creep specimen was calculated and considered to be the modulus of rupture of the

creep specimen. The beams were rejected if the moduli of rupture of the controls were not nearly the same. As noted later, this value is not necessarily correct, because of the defects inherent in wood. It was decided that the simple average of the controls was perhaps just as accurate as more elaborate weighting methods. Variations in growth structure would influence the result as inexorably with any type of average. There has been little or no work published on this aspect of the determination of properties.

A predetermined percentage of the load calculated for the average modulus of rupture was placed on the creep specimen. Since the weight placed on the beam only approximated the calculated weight, the percentage of the average modulus of rupture for the actual load was then calculated. This value is used in all subsequent data manipulations and referred to as the "percentage of the average modulus of rupture" or, more simply, as the "stress level."

The influence of temperature and humidity on a loaded beam is shown in figure 5. A phenomenon frequently observed is the "tension failure." This is not always a visual phenomenon; often it is merely a distinctly audible crack accompanied by a perceptible increase in the beam deflection. Creep rate will often be very great immediately after the tension failure, but may, in a reasonably short time, decrease to the creep rate prior to the failure. Sometimes the crack will be accompanied by visible separation of fine fibers from the tension side of the beam. It is suggested that this is not a true tension failure, with destruction of the area under tension, but an internal readjustment which does nothing to disturb seriously the cross section of the beam.

The result of a large rise in temperature, or an increase in relative humidity, is an increase in the deflection. The immediate effect of temperature change on most static strength properties of dry wood is to decrease or increase the property $1/3$ to $1/2$ percent for each 1° rise or drop in temperature in the neighborhood of 70° F. Correspondingly, the change in static bending properties due to a change of 1 percent in moisture content is roughly 4 to 5 percent. The deflection behavior accompanying humidity changes can be at least partially attributed to the weakening influence of increases in moisture content on the outer fibers. The return of the atmosphere to normal is followed by gradual drying of the wood, and often a resumption of the original creep rate. If the creep rate returns to what it was before the disturbance, the amount of the increase is subtracted from each ordinate in order to provide sufficient points for describing the curve.

Since this was the first attempt to analyze all of the constant load data, all specimens were graphed. Deflection-time plots were prepared and all remarks made by observers noted on the graphs. The initial deflection and zero time were taken at the end of loading, since up to that time the load had been increasing. Smooth curves were drawn through the points except at

obvious discontinuities. The number of observations was, in most cases, more than sufficient to allow a curve to be drawn which accurately described the behavior of the specimen.

Consideration of the overall shape of the curves that generally had a primary stage, a point of inflection rather than a well-defined straightline secondary stage, and a wide variety of shapes after the point of inflection, led (after a few trials) to the use of the empirical power law formula for a description of the behavior of the creep specimens before the point of inflection was reached. The description of the curve after the point of inflection is probably not possible until more is known about the manner in which the beams fail under long-time loading.

Since a smooth curve had been easily drawn through the points, the curve was used for the calculation of the power law constants. The method used was an adaptation of one proposed by La Combe (13):

Let the form of the curve be

$$\epsilon = \epsilon_0 + at^m$$

Where $\underline{\epsilon}$ and \underline{t} are variable and $\underline{\epsilon}_0$, \underline{a} , and \underline{m} are constants; let the \underline{t} 's be chosen so that they form a geometric progression with the ratio \underline{r} . Then the terms are

$$t_1, t_2 = t_1 r, t_3 = t_1 r^2, \dots, t_n = t_1 r^{n-1}$$

For two consecutive values of \underline{t} ,

$$\epsilon_{n+1} = \epsilon_0 + at_{n+1}^m$$

$$\epsilon_n = \epsilon_0 + at_n^m$$

or

$$\Delta\epsilon = \epsilon_{n+1} - \epsilon_n = a(t_{n+1}^m - t_n^m) = at_n^m(r^m - 1)$$

taking logarithms

$$\log_{10} \Delta\epsilon = \log_{10} a(r^m - 1) + m \log_{10} t_n$$

a straight line in the variables $\log_{10} \Delta\epsilon$ and $\log_{10} t_n$ with slope \underline{m} and intercept $\log_{10} a(r^m - 1)$.

In summary, the required constants may be found by the following procedure. Choose a set of \underline{t} 's in geometric progression with a ratio \underline{r} , and tabulate them with their corresponding $\underline{\epsilon}$'s obtained from the curve. A series of values of $\log_{10} t$ and $\log_{10} \Delta\epsilon$ will be found which will fall nearly on a

straight line. For such a few points it is a simple matter to obtain the slope constant, \underline{m} , and the intercept constant, $\log_{10} a(r^m - 1)$, by least squares and from this obtain the slope constant, \underline{a} . Knowing these a series of $\underline{\epsilon}_0$'s can be calculated from the $\underline{\epsilon}$'s and \underline{t} 's that were originally chosen. The average of these is the constant $\underline{\epsilon}_0$, which is used in the equation

$$\epsilon = \epsilon_0 + at^m$$

In order to have all data homogeneous in time, the \underline{t} 's are all expressed in minutes by writing $(60 t)^m$ for \underline{t} in hours and $(1,440 t)^m$ for \underline{t} in days.

The various constants obtained from the equations were divided by the initial deflection due to loading, δ_0 . This procedure removed some of the variation due to specimen individuality.

Figures 6 through 11 are plots of the various parameters, $\frac{\epsilon_0}{\delta_0}$, $\frac{a}{\delta_0} \times 1,000$, and \underline{m} against stress level. Figures 12 through 17 are plots of stress levels against the deflection at the point of inflection, $\frac{\delta_{PI}}{\delta_0}$, the time at the point of inflection, and the minimum creep rate.

The point of inflection and the minimum creep rate were determined graphically. The trend lines were computed by the method of averages (48).

The trend lines for both equilibrium moisture contents are given on each graph for comparison purposes. The plotted points refer only to the solid line curve in each case.

Analysis of Data

Many factors can lead to difficulties in obtaining satisfactory data in creep experiments. The estimation of a modulus of rupture for the creep specimens destroys the compactness of the data by permitting unknown variations due to defects hidden in the structure of the specimen. Therefore, the actual short-time ultimate strength for the creep specimen is never known.

Figures 18 and 19 show the distribution of the stress levels with respect to times of failure under equilibrium moisture contents of 6 and 12 percent, respectively. The plots have the failing of all graphs with logarithmic axes--that of "pushing together" the values so that a range of 1 day at one end of the axis may occupy the same space as 2 or 3 years at the other end. Superposition of the figures shows much the same distribution of points for both, regardless of the 6 percent difference in moisture content. The trend lines indicate that there is little difference to time of failure at equilibrium moisture contents of 6 and 12 percent. The 10 specimens conditioned at 80° F. and 65 percent relative humidity appear to be randomly

scattered through the 75° F. and 64 percent relative humidity specimens, and there is no evidence that a 5° difference in conditioning temperature affected their life.

The equations for the trend lines are:

$$S.L. = 89 - 6 \log T_F \dots (6 \text{ percent moisture content})$$

$$S.L. = 90 - 6 \log T_F \dots (12 \text{ percent moisture content})$$

where S.L. is the stress level and T_F the time to failure after loading, in hours.

Figures 14 and 15 are plots of the stress level against the time to the point of inflection. This is a valuable point to be able to predict, since it is here that failure can be said to begin. Superposition of the graphs shows the points of the 6 percent plot falling among those of the 12 percent plot in a random manner. The points representing tests conducted at 80° F. and 65 percent relative humidity appear to be well scattered among those representing tests at 75° F. and 64 percent relative humidity. The 5° temperature difference apparently has little effect. The equations for the trend lines are:

$$S.L. = 88 - 6 \log T_{PI} \dots (6 \text{ percent moisture content})$$

$$S.L. = 91 - 7 \log T_{PI} \dots (12 \text{ percent moisture content})$$

where S.L. is the stress level and T_{PI} the time at point of inflection.

The lines intersect at roughly the 70 percent stress level. This intersection possibly has little meaning, since, in addition to the natural spread in the data, the point of inflection is difficult to locate accurately. The differences should probably be ignored and, within the range of 6 to 12 percent, moisture content may be considered to have little effect on time to point of inflection.

In figures 16 and 17, stress level is plotted against the minimum creep rate. This is the creep rate occurring at the time of the point of inflection. The equations for these figures are:

$$S.L. = 59 + 6 \log \dot{\epsilon}_{\min} \dots (6 \text{ percent moisture content})$$

$$S.L. = 56 + 7 \log \dot{\epsilon}_{\min} \dots (12 \text{ percent moisture content})$$

Although these lines intersect, they do so at an even smaller angle than those in figures 14 and 15. The error involved in measuring the tangent to the curve may be large, and it is surprising that the data are not more

erratic. On this basis, it appears reasonable to neglect the crossing of the lines and assume that there were only small differences in minimum creep rates between specimens at the two moisture contents.

The deflection at the point of inflection expressed in terms of initial deflection, δ_0 , plotted against stress level is shown in figures 12 and 13. The points for the 6 and 12 percent moisture content levels fall into distinctly separate areas, in contrast to the plotted data previously shown. At any stress level, the ratio for the specimens at 12 percent moisture content was approximately 1.21 times the ratio for those at 6 percent moisture content. The equations of the trend lines are:

$$S.L. = 196 - 92 (\delta_{PI}/\delta_0) \dots (6 \text{ percent moisture content})$$

$$S.L. = 222 - 93 (\delta_{PI}/\delta_0) \dots (12 \text{ percent moisture content})$$

The remaining graphs are concerned with the relations between the stress level and the various constants in the power law equation. Although these constants have no basis in physical reality, correlation with the conditions of the experiment may be valuable for prediction purposes or for relating other factors.

The three constants determine the shape and location of the curve. The constant, ϵ_0 , is similar to but not the same as the instantaneous deflection in that it moves the intersection of the curve with the y -axis up or down. The constant, a , can be considered to be a magnification factor. The constant, m , provides information on the creep rate.

A plot of stress level and ϵ_0/δ_0 (figs. 6 and 7) indicates that ϵ_0/δ_0 is almost independent of stress level. The 80° F. and 65 percent relative humidity points are well scattered through the other 12 percent moisture content points. The near perpendicularity of the lines may be seen from the slopes of the equations, which are:

$$S.L. = 812 - 733 (\epsilon_0/\delta_0) \dots (6 \text{ percent moisture content})$$

$$S.L. = 660 - 586 (\epsilon_0/\delta_0) \dots (12 \text{ percent moisture content})$$

Figures 10 and 11 show the relations between m and the stress level. The relationship for 6 percent moisture content is practically insensitive to stress level (within approximately 3 minutes of arc of being perpendicular), and has an average value of 0.35. The experimental errors and material variations could easily account for the slight deviation from the vertical.

The relationship for 12 percent moisture content is more difficult to explain. Undoubtedly, much of the deviation of the line is due to the influence of the points in the upper right-hand part of the graph. If these

were eliminated, the trend line would probably approach the vertical with a constant m value of about one-third. The small difference in room temperatures may have influenced the results, but this is impossible to show from the data.

It is interesting to note that the value of the exponent, m , has been found to be nearly independent of stress (given the same material and temperatures) for iron, steel, several pure metals, and some reinforced plastics. In addition, it has been found to be approximately equal to one-third for various materials, such as copper, lead, Ni-Cr-Mo steel, and concrete.

The equations for the lines are:

$$S.L. = -333 + 1,175 m \dots (6 \text{ percent moisture content})$$

$$S.L. = 23 + 151 m \dots (12 \text{ percent moisture content})$$

Figures 8 and 9 show the graph of stress level and $\log \left(\frac{a}{\delta_o} \times 1,000 \right)$. The quantity increases for both moisture contents as the stress level increases and is greater for the 12 percent moisture content data. The 80° F. and 65 percent relative humidity points are distributed evenly through the 75° F. and 64 percent relative humidity points.

The equations of the trend lines are:

$$S.L. = 49 + 22 \log \left(\frac{a}{\delta_o} \times 1,000 \right) \dots (6 \text{ percent moisture content})$$

$$S.L. = 32 + 28 \log \left(\frac{a}{\delta_o} \times 1,000 \right) \dots (12 \text{ percent moisture content})$$

For the various relations that have been considered above, the limits of the values for the specimens at 12 percent moisture content appear to be a little wider in general than the limits for those at 6 percent. This can be observed in the slightly larger scatter of the points in the 12 percent graphs as opposed to the 6 percent graphs.

Part of the spread may be due to the greater difficulties that arose in the operation of the air conditioner for the 12 percent equilibrium moisture content room during the course of these experiments. A wide spread characterizes the data of these experiments in particular and of wood in general. Much of it is due to the natural variation found in clear wood specimens, but many serious defects also develop during growth, and these are hidden until the wood is tested. The method of determining the stress level from the controls may provide more inaccuracies, which increase the scatter of the data.

Conclusions

The following conclusions are based on the reported test conditions and test data:

1. The creep behavior up to the point of inflection can be satisfactorily described by an empirical expression of the form, $\epsilon = \epsilon_0 + at^m$. The constant, m , has a value of about one-third and is probably independent of stress level and moisture content within the range studied. The constant $(\frac{a}{\epsilon_0} \times 1,000)$, should increase with an increase in stress level or moisture content.
2. The time to failure will increase as the stress level is decreased and is independent of moisture content for the levels used in these experiments.
3. The time to the point of inflection of the creep curve can be used to predict the start of failure of the beam. This time is dependent upon stress level and independent of the moisture content at the levels employed in these tests.
4. Since all specimens that were tested failed, the creep limit, if it exists, must be below the 60 percent stress level.
5. Increasing the moisture content level from approximately 6 percent to approximately 12 percent appears to increase the ratio of deflection for any given stress level by a factor of approximately 1.2.
6. Any effects arising from small temperature differences cannot be estimated from the data obtained.
7. The results of these tests and similar tests can be of value to the engineer and the designer in estimating the behavior of structures under long-time loading.

Literature Cited

1. American Society for Metals.
1957. Creep and Recovery, Cleveland: American Society for Metals, 372 pp.
2. American Society for Testing Materials.
1958. Report of the Joint ASTM-ASME Committee on the Effect of Temperature on the Properties of Metals, pp. 23-24.
3. American Society for Testing Materials.
1955. Standard Method for Testing Small Clear Specimens of Timber. 1955 Book of ASTM Standards, Part 4. Specification D143-52.
4. Andrade, E. N. da C.
1914. The Flow in Metals Under Large Constant Stresses. Proceedings of the Royal Society, Vol. 90, p. 329.
5. Armstrong, L. D.
1953. Short Term Creep Tests on Air-Dry Wooden Beams. Division of Forest Products (Sub. Proj. T.P. 16-1), Australian CSIRO. Progress Report No. 2, September.
6. Barkas, W. W.
1949. The Swelling of Wood Under Stress. Department of Scientific and Industrial Research, Forest Products Research, London. 103 pp.
7. Boltzmann, L.
1876. Zur Theorie der Elastischen Nachwirkung. Pogg. Ann. Physik, Vol. 7, p. 624.
8. Buffon, G. L. L. De.
1740. Experiences sur la Force du Bois. Paris L'Academie Royale des Sciences. Histoire et Memoires, Vol. 292. Also Vol. 453 (1741).
9. Carey, R. H., and Oskin, E. T.
1956. The Prediction of Long-Time Stress-Rupture Data From Short-Time Tests. SPE Journal, Vol. 12, No. 3, p. 21.
10. Cottrell, A. H.
1953. Dislocations and Plastic Flow in Crystals. Oxford University Press, London. 223 pp.
11. Crussard, C.
1946. Le Role des Joints Intergranulaires dans la Deformation des Metaux. Application au Fluage et a la Fatigue. Revue de Metallurgie, Vol. 43, p. 307.

12. Davis, E. A.
1943. The Creep and Relaxation of Oxygen-Free Copper. *Journal of Applied Mechanics*. Vol. 10, p. A-101.
13. de La Combe, M. J.
1939. Un Mode de Representation des Courbes de Fluage. *Revue de Metallurgie*, Vol. 36, pp. 178-188.
14. Draffin, J. O., and Muhlenbruch, C. W.
1937. The Mechanical Properties of Balsa Wood. *Proc., American Society for Testing Materials*, Vol. 37, Pt. II, pp. 582-587.
15. Filon, L. N. G., and Jessop, H. T.
1923. On the Stress-Optical Effect in Transparent Solids Strained Beyond the Elastic Limit. *Philosophical Trans. of the Royal Society of London*. Ser. A., Vol. 223, pp. 89-125.
16. Findley, W. N.
1944. Creep Characteristics of Plastics. *American Society for Testing Materials, Symposium in Plastics*. p. 118.
17. Findley, W. N., and Khosla, G.
1956. An Equation for Tension Creep of Three Unfilled Thermoplastics. *SPE Journal*, Vol. 12, No. 12, p. 20.
18. Flory, P. J.
1953. *Principles of Polymer Chemistry*. Cornell University Press, Ithaca, N. Y. 672 pp.
19. Fluck, P. G., and Washa, G. W.
1958. Creep of Plain and Reinforced Concrete. *Journal of the American Concrete Institute*, Vol. 29, No. 10.
20. U. S. Forest Products Laboratory.
1955. *Wood Handbook*. U. S. Dept. of Agric. Agriculture Handbook No. 72. 528 pp., illus.
21. Glasstone, S., Laidner, K. J., and Eyring, H.
1941. *The Theory of Rate Processes*. McGraw-Hill, New York. 611 pp.
22. Goldfein, S.
1954. Time-Temperature and Rupture Stresses in Reinforced Plastics. *Modern Plastics*, Vol. 32, p. 148, December.
23. Graf, O.
1938. Tragfähigkeit der Bauhölzer und der Holzverbindungen. *Mitt. Fachaussch. Holzfr.*, H. 20 S. 40. Berlin 1938 (Reported in Reference 29, p. 866).

24. Gross, Bernhard.
1953. Mathematical Structure of the Theories of Visco-Elasticity. Hermann et Cie. Editeurs, Paris. 74 pp.
25. Heimerl, S. S., and Haferd, A. M.
1954. Time-Temperature Parameters and An Application to Rupture and Creep of Aluminum Alloys. National Advisory Committee for Aeronautics Technical Note 3195. June.
26. Kauzmann, W.
1941. Flow of Metals From the Standpoint of the Chemical Rate Theory. Trans. Amer. Institute of Min. and Met. Engr., Vol. 143, pp. 57-81.
27. Kingston, R. S. T.
1949. Creep in Initially Green Beams. Australian CSIRO, Division of Forest Products, Exp. T.P. 16-1/1. Progress Report No. 1, June.
28. Kingston, R. S. T., and Armstrong, L. D.
1951. Creep in Initially Green Wooden Beams. Australian Journal of Applied Science, Vol. 2, p. 306.
29. Kollmann, Franz.
1951. Technologie des Holzes und der Holzwerkstoffe. Erster Band, Springer-Verlag, Berlin. 1,050 pp.
30. Larson, F. R., and Miller, J.
1952. A Time-Temperature Relationship for Rupture and Creep Stresses. Trans. American Society of Mechanical Engineers, Vol. 74, No. 5, pp. 765-775.
31. Lea, F. M., and Lee, C. R.
1947. Shrinkage and Creep in Concrete. Proc., Symposium on the Shrinkage and Cracking of Cementative Materials. Society of Chemical Industry, London.
32. Leaderman, H.
1943. Elastic and Creep Properties of Filamentous Materials and Other High Polymers. The Textile Foundation, Washington. 278 pp.
33. Lorman, W. R.
1940. The Theory of Concrete Creep. Proc., American Society for Testing Materials, Vol. 40, pp. 1082-1102.
34. McHenry, Douglas.
1943. A New Aspect of Creep in Concrete and Its Application to Design. Proc., American Society for Testing Materials, Vol. 43, pp. 1069-1087.

35. McVetty, P. G.
1934. Working Stresses for High Temperature Service. Mechanical Engineering, Vol. 56, pp. 149-154, March.
36. Manjoine, M. J., and Mudge, W. L.
1954. Creep Properties of Annealed Unalloyed Zirconium. Proc. American Society for Testing Materials, Vol. 54, pp. 1050-1067.
37. Manson, S. S., and Haferd, A. M.
1952. A Linear Time-Temperature Relation for Extrapolation of Creep and Stress in Rupture Data. National Advisory Committee for Aeronautics Technical Note 2890, March.
38. Merideth, R.
1953. Mechanical Properties of Wood and Paper. Interscience Publishing Co., New York. 298 pp.
39. Nadai, A., and McVetty, P. G.
1943. Hyperbolic Sine Chart for Estimating Working Stresses of Alloys at Elevated Temperatures. Proc. American Society for Testing Materials, Vol. 43, pp. 735-748.
40. National Lumber Manufacturers Association.
1953. National Design Specifications for Stress-Grade Lumber and Its Fastening.
41. National Physical Laboratory.
1956. Creep and Fracture of Metals at High Temperatures. National Physical Laboratory, London. 419 pp.
42. Neville, A. M.
1955. Theories of Creep in Concrete. ACI Journal, Vol. 27, No. 1, p. 47.
43. Ott, Emil.
1943. Cellulose and Cellulose Derivatives. Interscience Publishing Co., New York. 1176 pp.
44. Parent.
1707. Experiences pour Connaitre la Resistance des Bois de Chene et de Sapin. L'Academie Royale des Sciences, Paris. Histoire et Memoires, 512.
45. Pickett, G.
1942. The Effect of Change in Moisture-Content on the Creep of Concrete Under a Sustained Load. ACI Journal, Proc., Vol. 38, pp. 333-355.

46. Pickett, G.
1946. Shrinkage Stresses in Concrete. ACI Journal, Proc., Vol. 42, pp. 165-204, January; pp. 361-398, February.
47. Rotherham, L. A.
1951. Creep of Metals. Institute of Physics, London. 80 pp.
48. Scarborough, J. B.
1930. Numerical Mathematical Analysis. The Johns Hopkins Press, Baltimore. 416 pp.
49. Schmidt, A. X., and Marlies, C. A.
1948. Principles of High Polymer Theory and Practice. McGraw-Hill, New York. 743 pp.
50. Shank, J. R.
1935. The Mechanics of Plastic Flow of Concrete. ACI Journal, Proc., Vol. 32, pp. 149-180, November-December.
51. Smith, George.
1950. Properties of Metals at High Temperatures. McGraw-Hill, New York. 401 pp.
52. Straub, L. G.
1931. Plastic Flow in Concrete Arches. Proc. American Society of Chemical Engineers, Vol. 95, p. 613.
53. Sturm, R. G., Dumont, C., and Howell, F. M.
1936. A Method of Analyzing Creep Data. Journal of Applied Mechanics, Vol. 3, No. 2, pp. A62-A66.
54. Sugiyama, Hideo.
1957. The Creep Deflection of Wood Subjected to Bending Under Constant Loading. Trans., Architectural Inst. of Japan. No. 55, pp. 60-70, February.
55. Sugiyama, Hideo.
1956. The Effect of Loading Time on the Bending Strength and Stiffness of Wood. Trans., Architectural Inst. of Japan. No. 52, March. (Forest Products Laboratory Translation No. 324, March, 1957.)
56. Sully, A. H.
1949. Metallic Creep. Butterworths Scientific Publications, London. 278 pp.
57. Sully, A. H., Cale, G. N., and Willoughby, G.
1948. Nature, London, 162, p. 411.

58. Tiemann, H. D.
1909. Some Results of Dead Load Bending Tests of Timber by Means of a Recording Deflectometer. Proc., American Society for Testing Materials, Vol. 9, pp. 534-548.
59. Tiemann, H. D.
1951. Wood Technology. Pitman Publishing Co., New York. 396 pp.
60. Vorreiter, Leopold.
1949. Holztechnologisches Handbuch. Verlag Georg Fromme and Co., Vienna. 548 pp.
61. Washa, George.
1955. Volume Changes and Creep. Significance of Tests and Properties of Concrete and Concrete Aggregates. Spec. Tech. Pub. No. 169, American Society for Testing Materials.
62. Weaver, S. H.
1936. The Creep Curves and Stability of Steels at Constant Stress and Temperature. Trans., American Society of Mechanical Engineers, Vol. 58, p. 745.
63. Wood, L. W.
1947. Behavior of Wood Under Continued Loading. Engr. News Record, Vol. 139, No. 24, pp. 108-111.
64. Wood, L. W.
1951. Relation of Strength of Wood to Duration of Load. Forest Products Laboratory Report No. 1916, December.

Table 1.--The distribution of the bending tests of
the control and creep specimens

Stress level ¹	Number of tests completed at--					
	75° F., 64 per- cent relative humidity		80° F., 65 per- cent relative humidity		80° F., 30 per- cent relative humidity	
	Creep specimen	Control specimen	Creep specimen	Control specimen	Creep specimen	Control specimen
Per- cent						
95	5	10	9	18
90	5	10	4	8	8	16
85	6	12	9	18
80	5	10	2	4	9	18
75	6	12	8	16
70	5	10	4	8	5	10
65	5	10	5	10
60	4	8	5	10
Totals	41	82	10	20	58	116

¹Stress level is the predetermined percentage of the average modulus of rupture computed from the moduli of rupture of the two control beams.

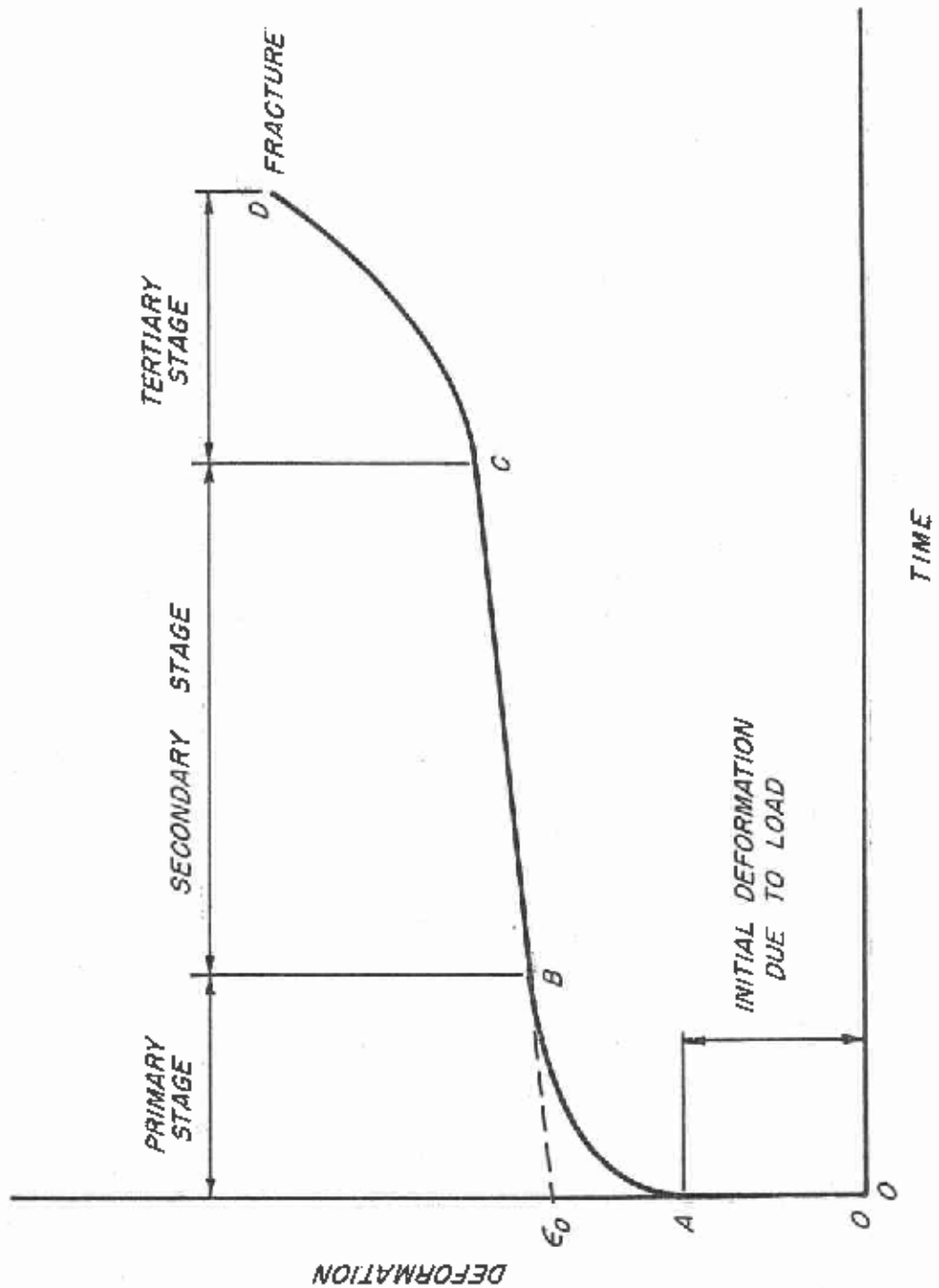


Figure 1. --Idealized constant-load creep curve.

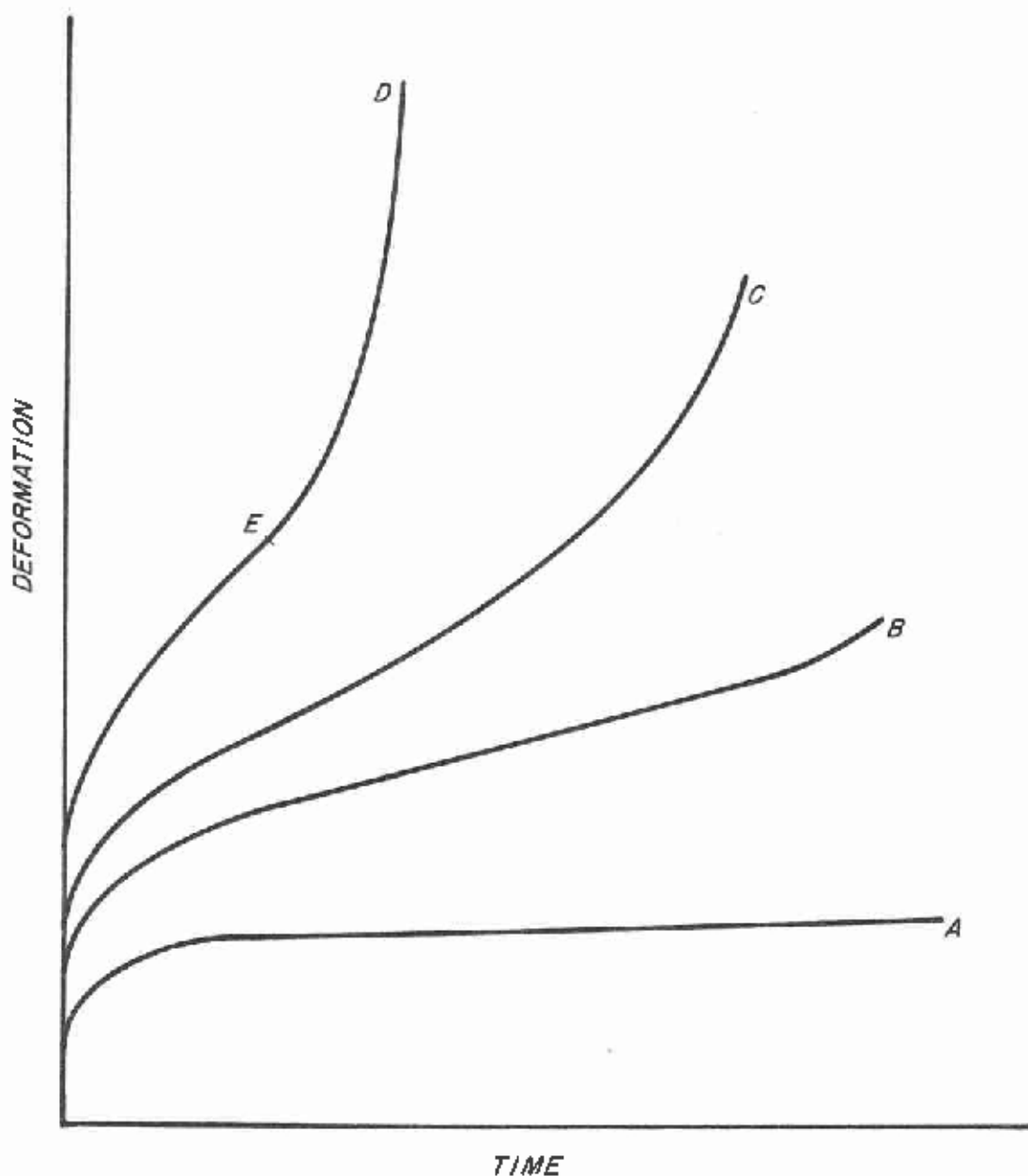


Figure 2. --Variation of the creep deformation-time relationship with load and temperature (after Cottrell (3)). Load or temperature of Curve A is lower than that of Curve D.

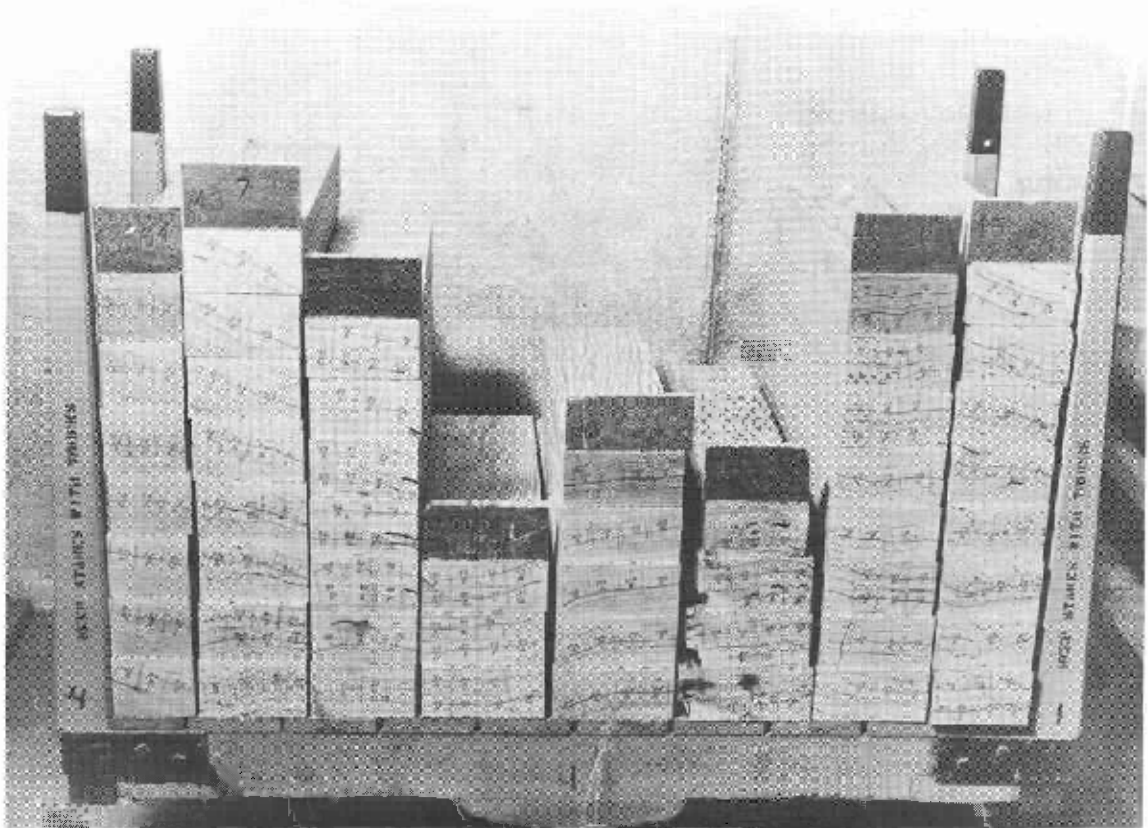


Figure 3.--View of several flat-sawn Douglas-fir planks used in the creep tests. The planks were cut into 22-inch lengths, and the locations of the ring-matched control and creep specimens were marked in pencil on the ends of these lengths.

Z M 60881 F



Figure 4.--A typical test frame containing four creep specimens under constant load. The load was applied through an iron stirrup that terminated in a wood platform holding the load of bars or bags of shot. The beams were simply supported on steel knife-edges and rollers. Deflections were shown directly on dial indicators. Not shown is the free-standing protective frame surrounding the stand.

Z M 80898 F

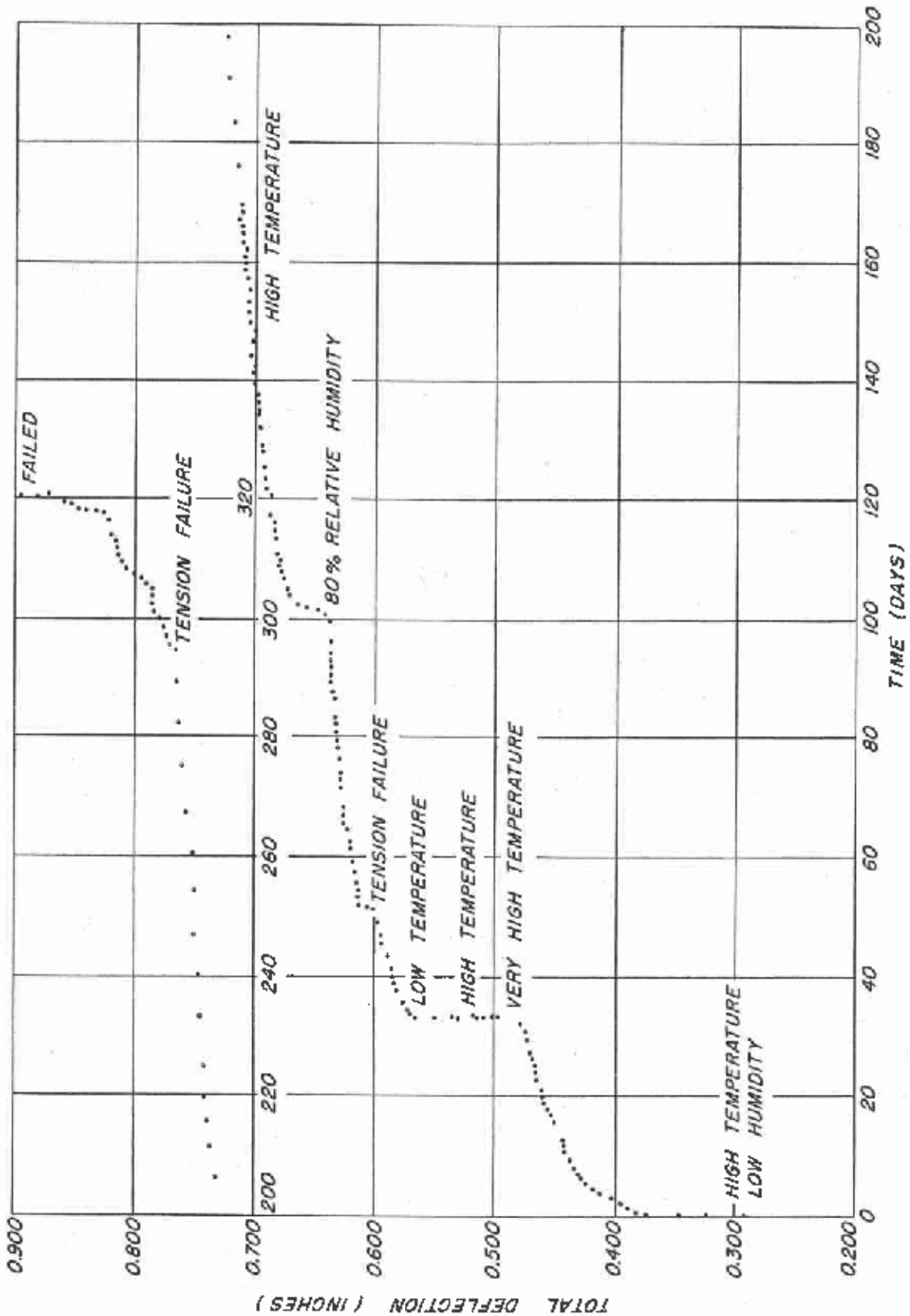


Figure 5.--Creep curve showing the effects of tension failure and of temperature and humidity changes occurring during test of a beam at 12 percent moisture content loaded to 65 percent of its estimated modulus of rupture.

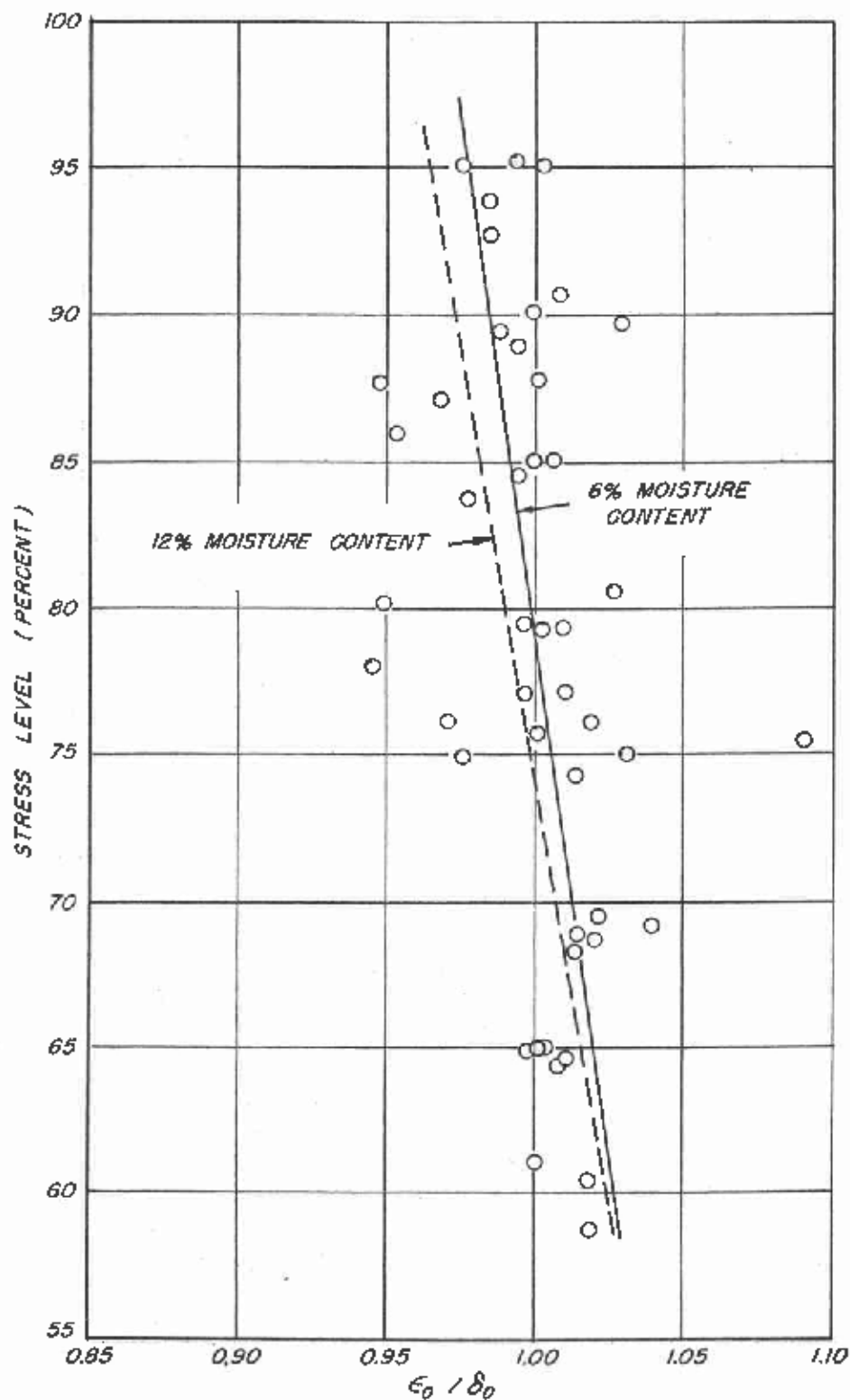


Figure 6.--Relationship between stress level and the ratio ϵ_0 / δ_0 at 6 percent moisture content.

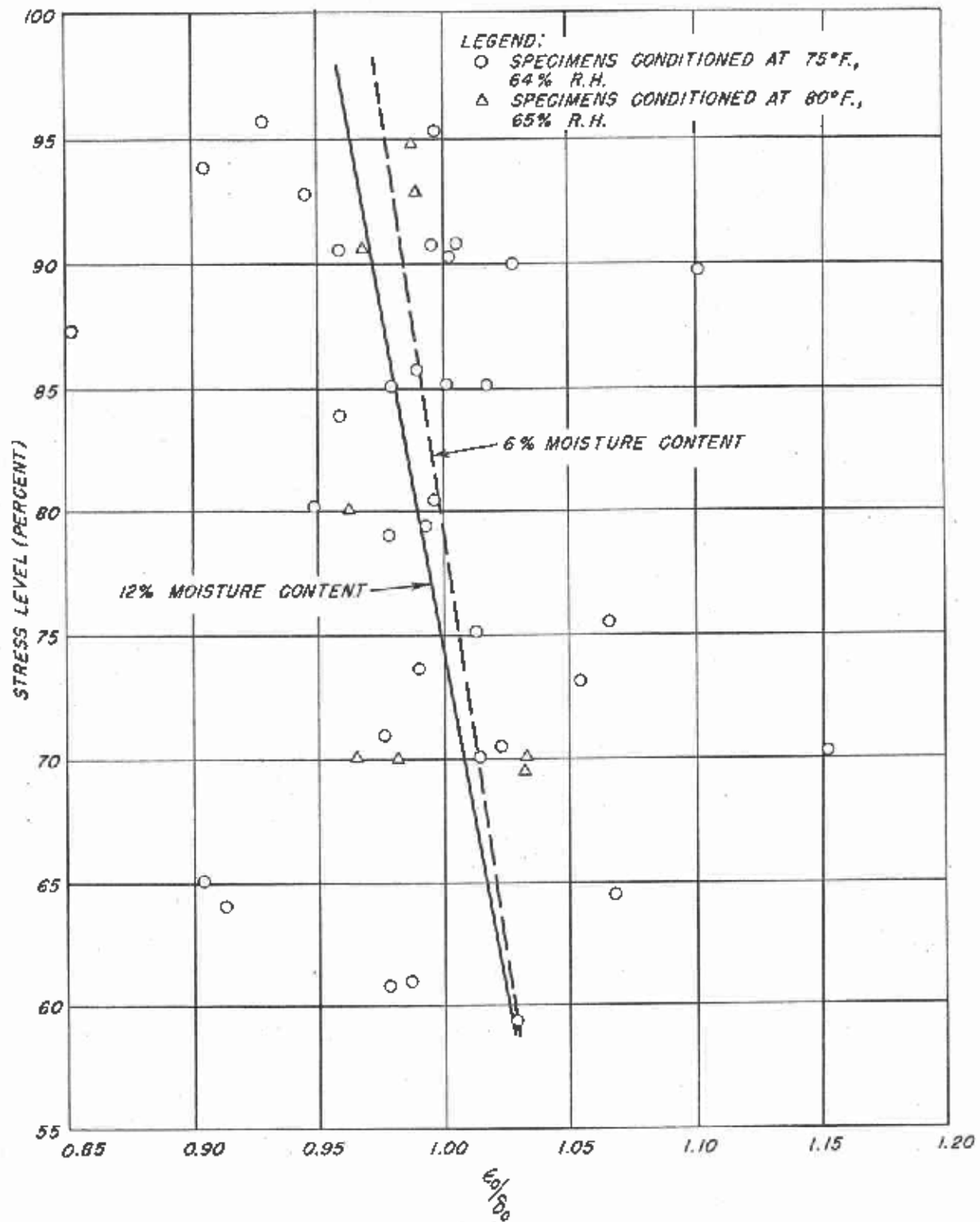


Figure 7. --Relationship between stress level and the ratio ϵ_0/δ_0 at 12 percent moisture content.

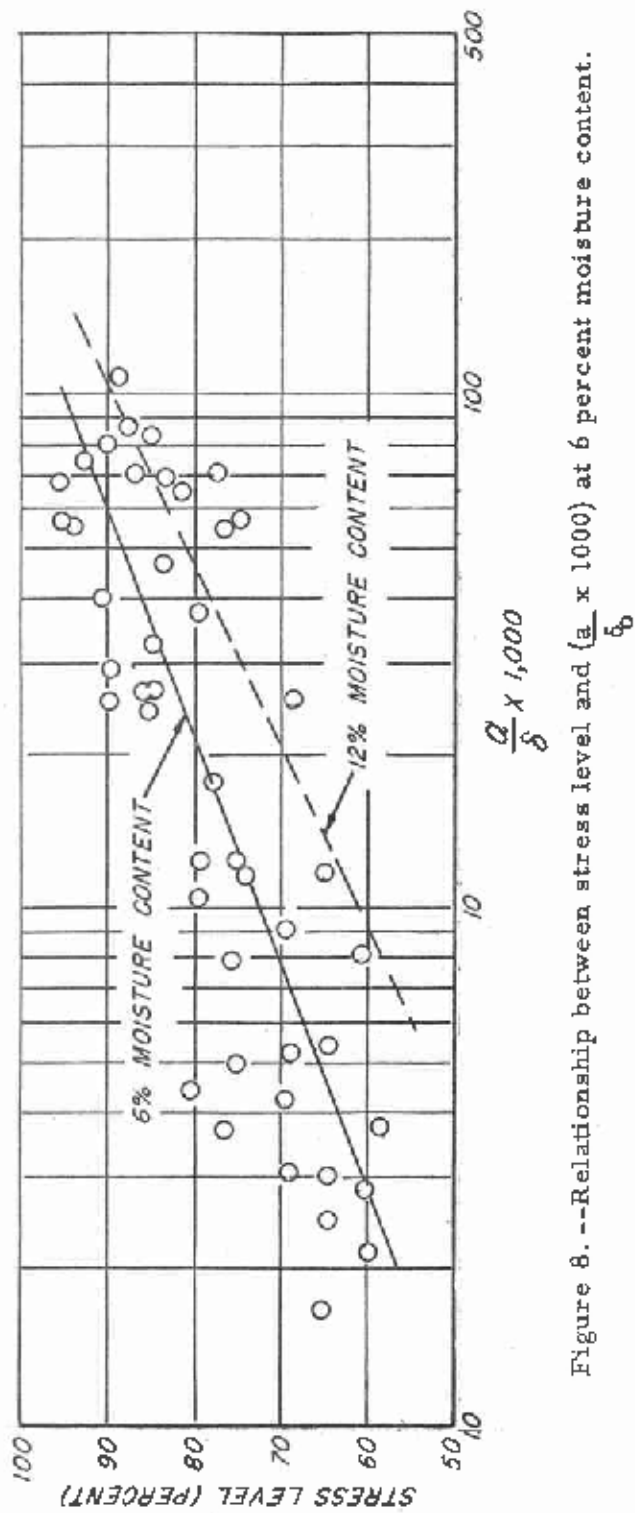


Figure 8. --- Relationship between stress level and $\left(\frac{a}{b} \times 1000\right)$ at 6 percent moisture content.

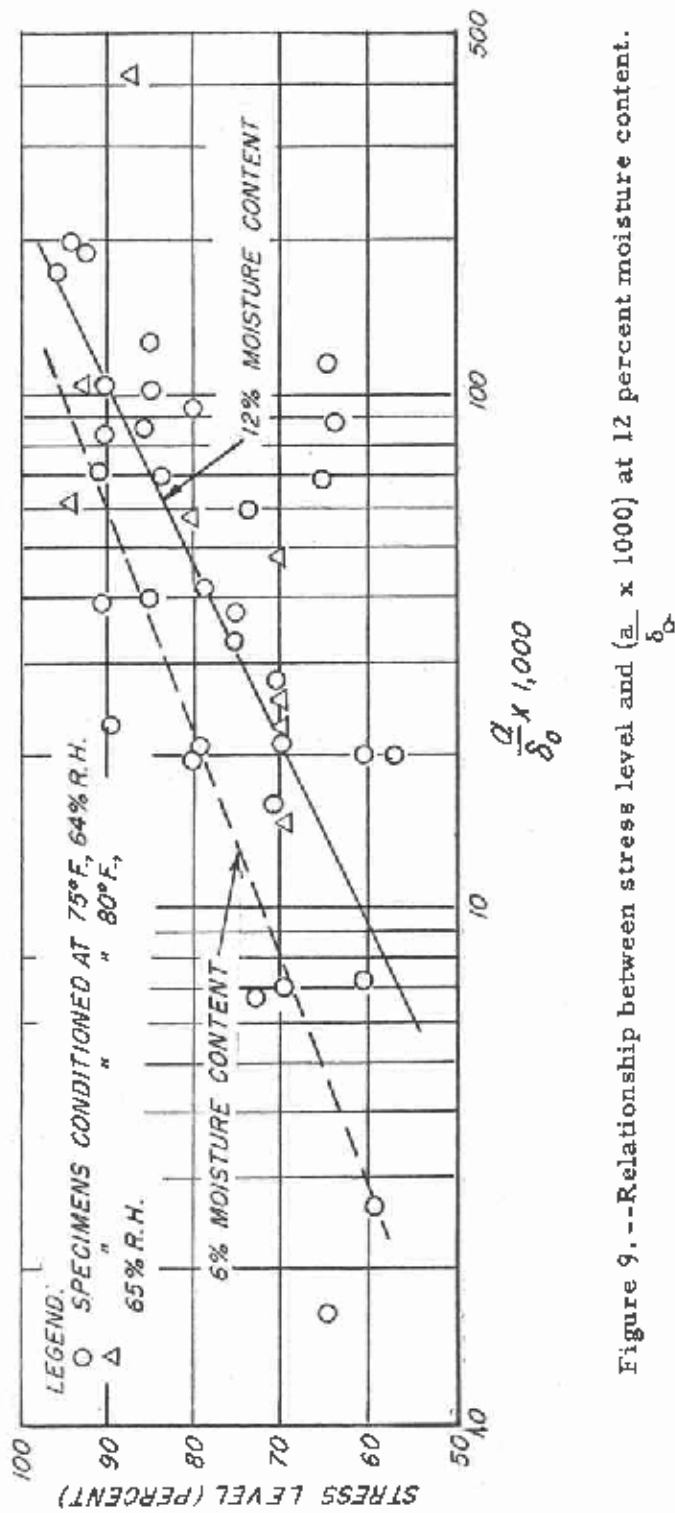


Figure 9. --- Relationship between stress level and $\left(\frac{a}{b} \times 1000\right)$ at 12 percent moisture content.

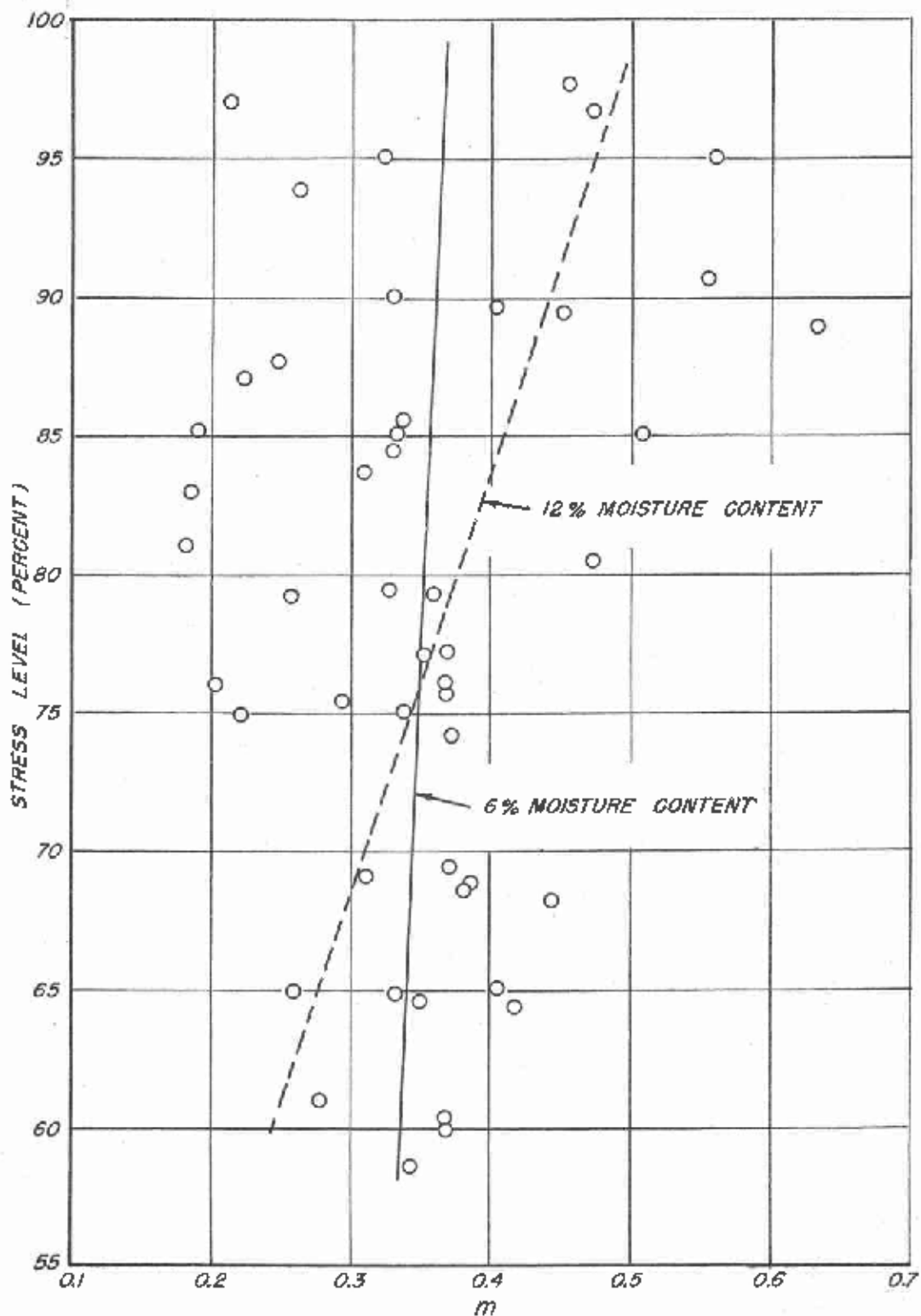


Figure 10. -- Relationship between stress level and m at 6 percent moisture content.

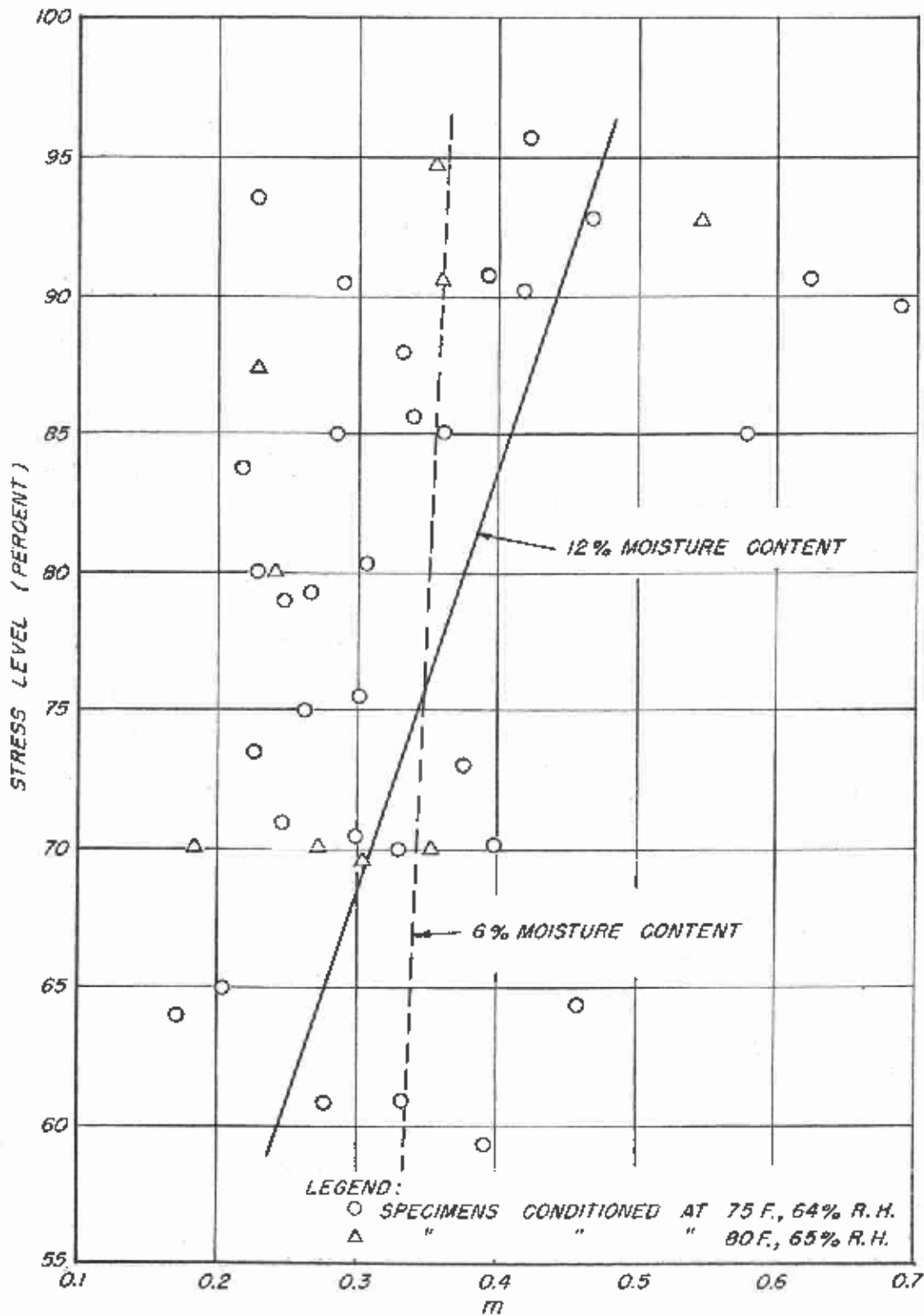


Figure 11. --Relationship between stress level and m at 12 percent moisture content.

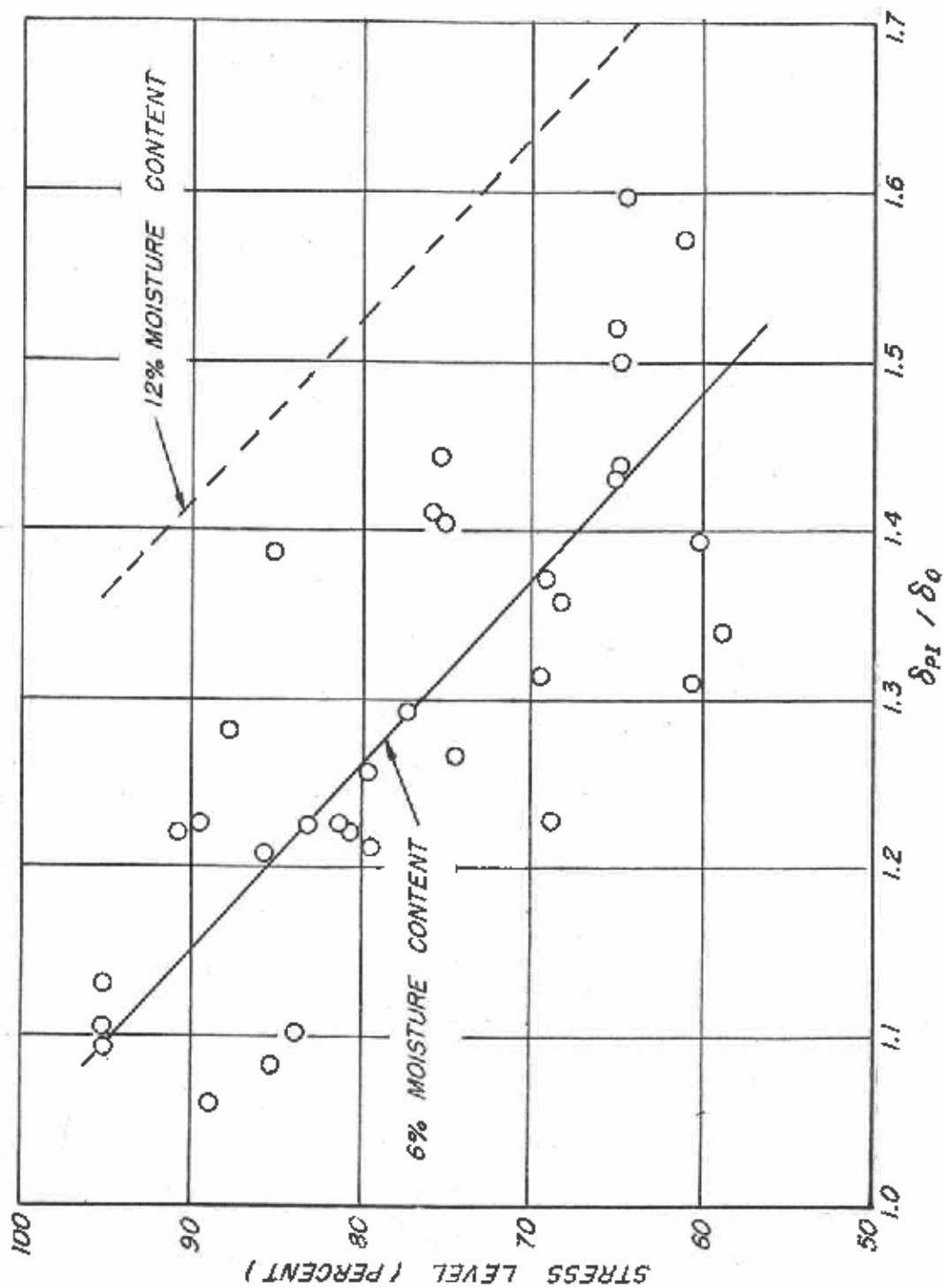


Figure 12. -- Relationship between stress level and $\delta \pi / \delta \sigma_0$ at 6 percent moisture content.

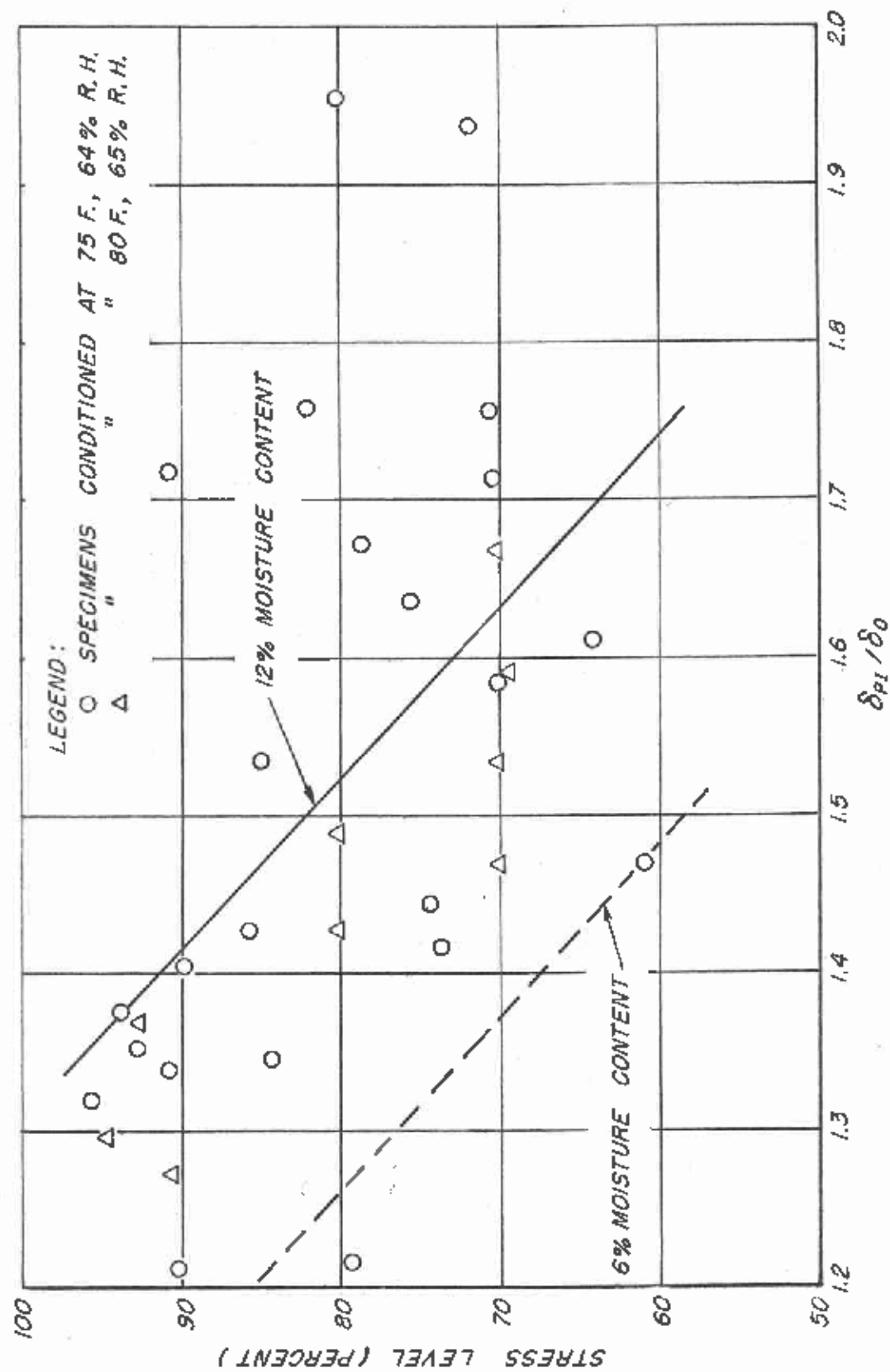


Figure 13. -- Relationship between stress level and the ratio $\delta P_I / \delta \sigma$ at 12 percent moisture content.

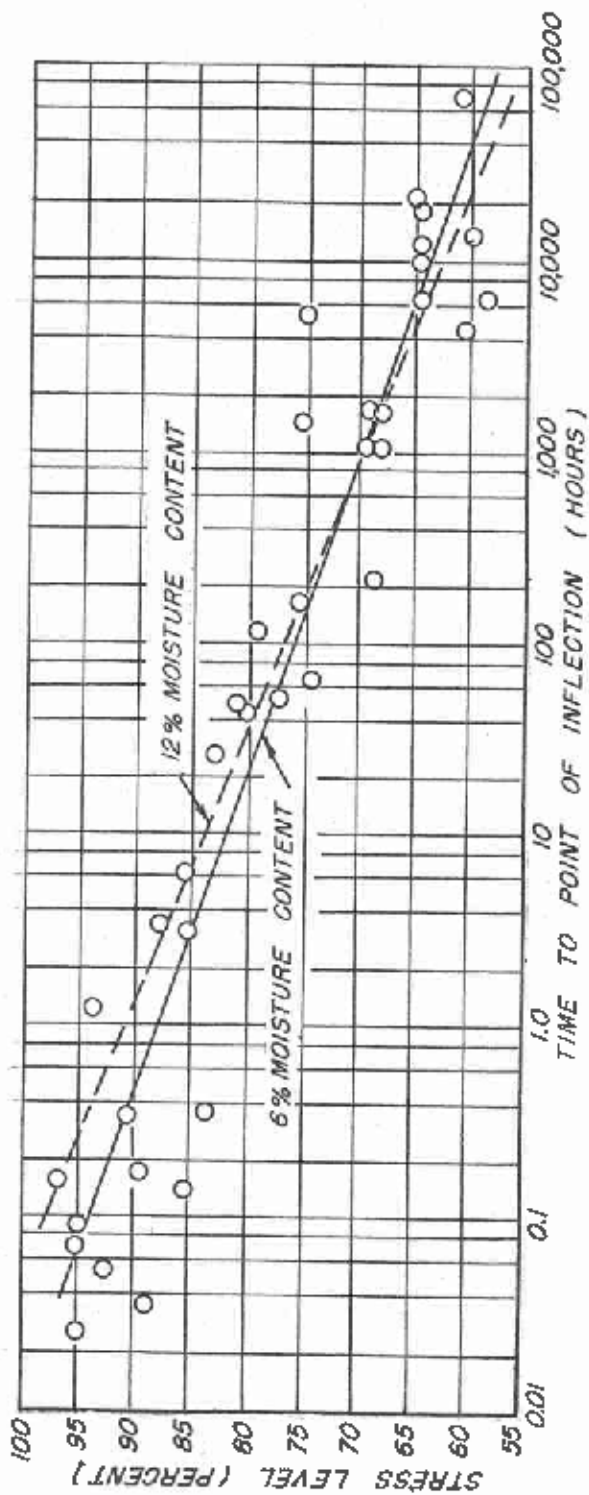


Figure 14.--Relationship between stress level and time to point of inflection at 6 percent moisture content.

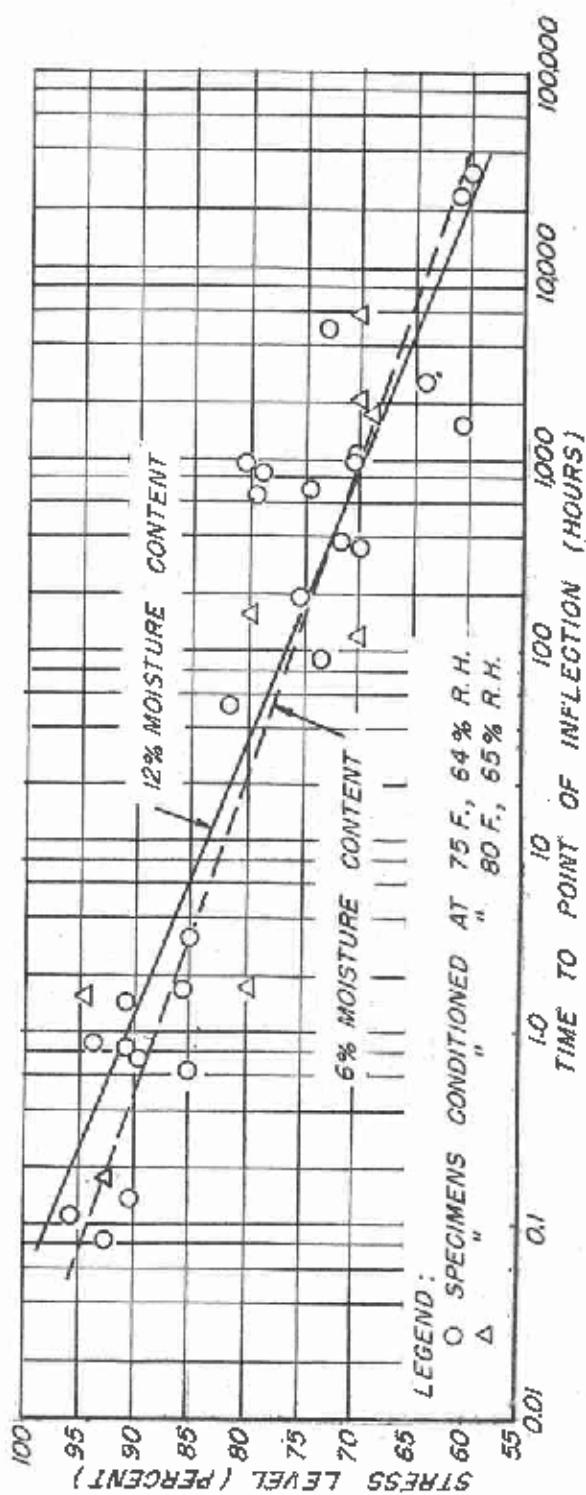


Figure 15.--Relationship between stress level and time to point of inflection at 12 percent moisture content.

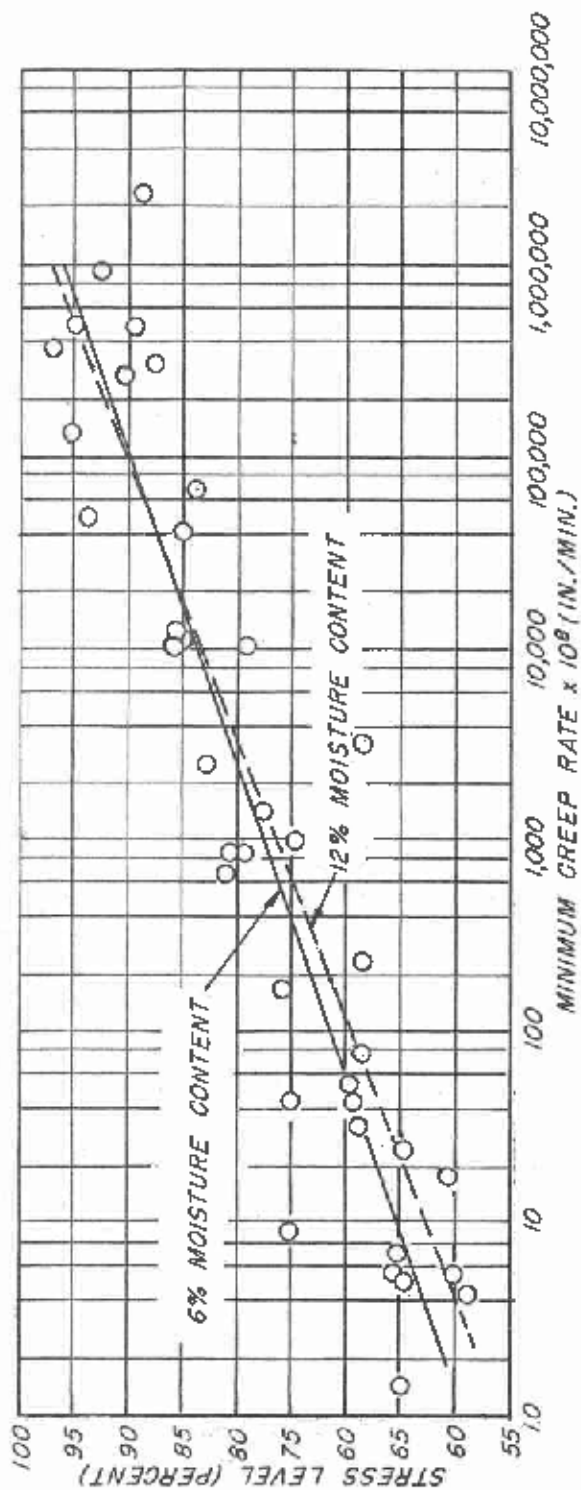


Figure 16. -- Relationship between stress level and minimum creep rate at 6 percent moisture content.

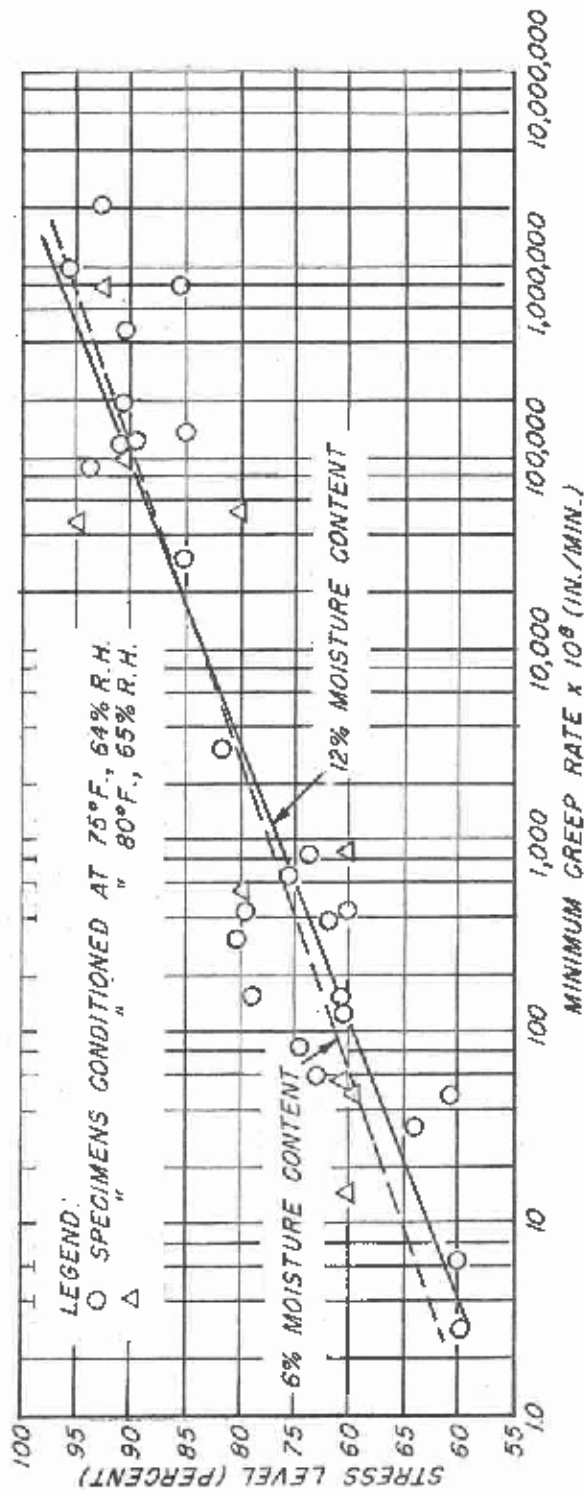


Figure 17. -- Relationship between stress level and minimum creep rate at 12 percent moisture content.

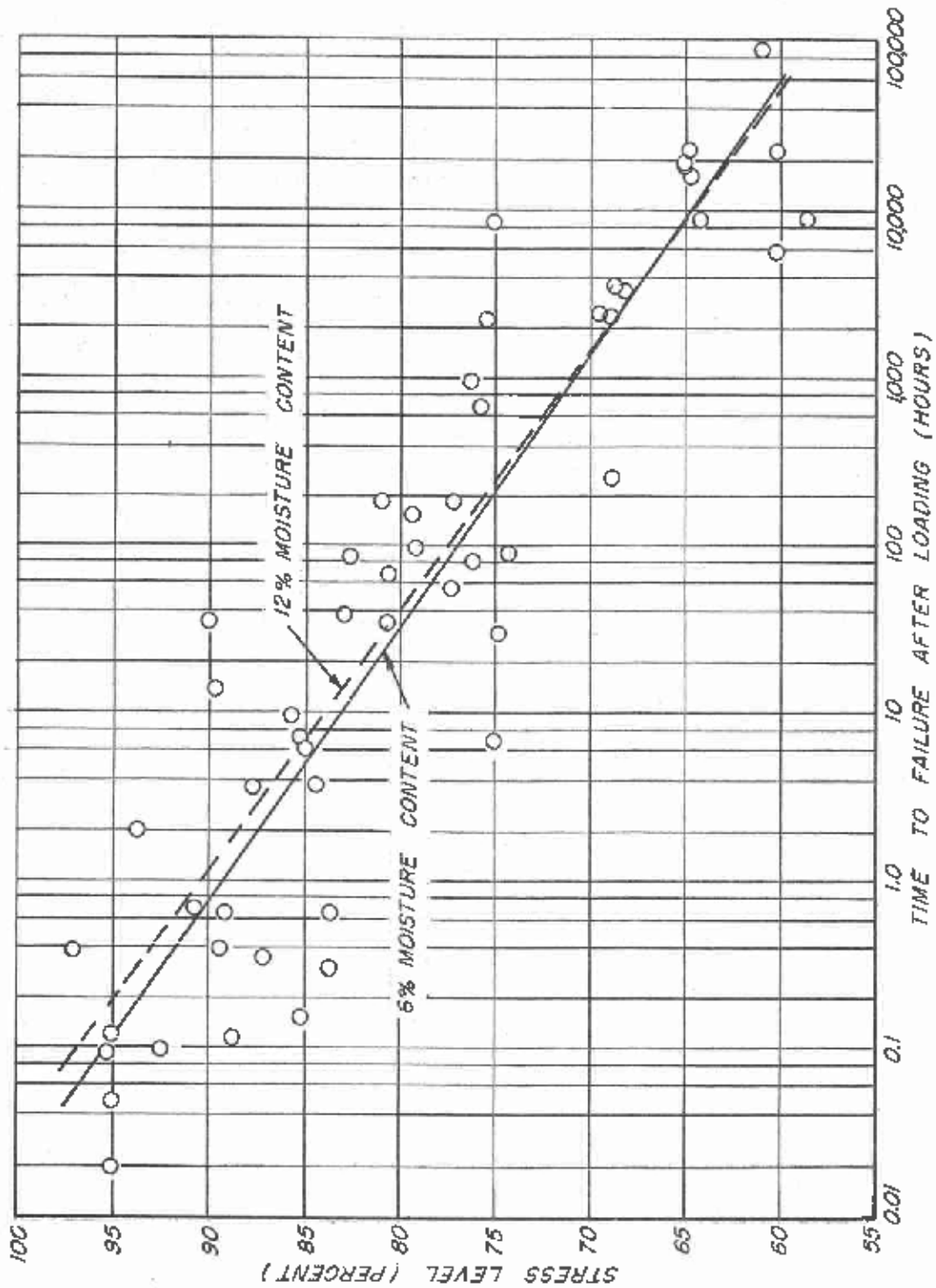


Figure 18. --Relationship between stress level and time to failure after loading at 6 percent moisture content.

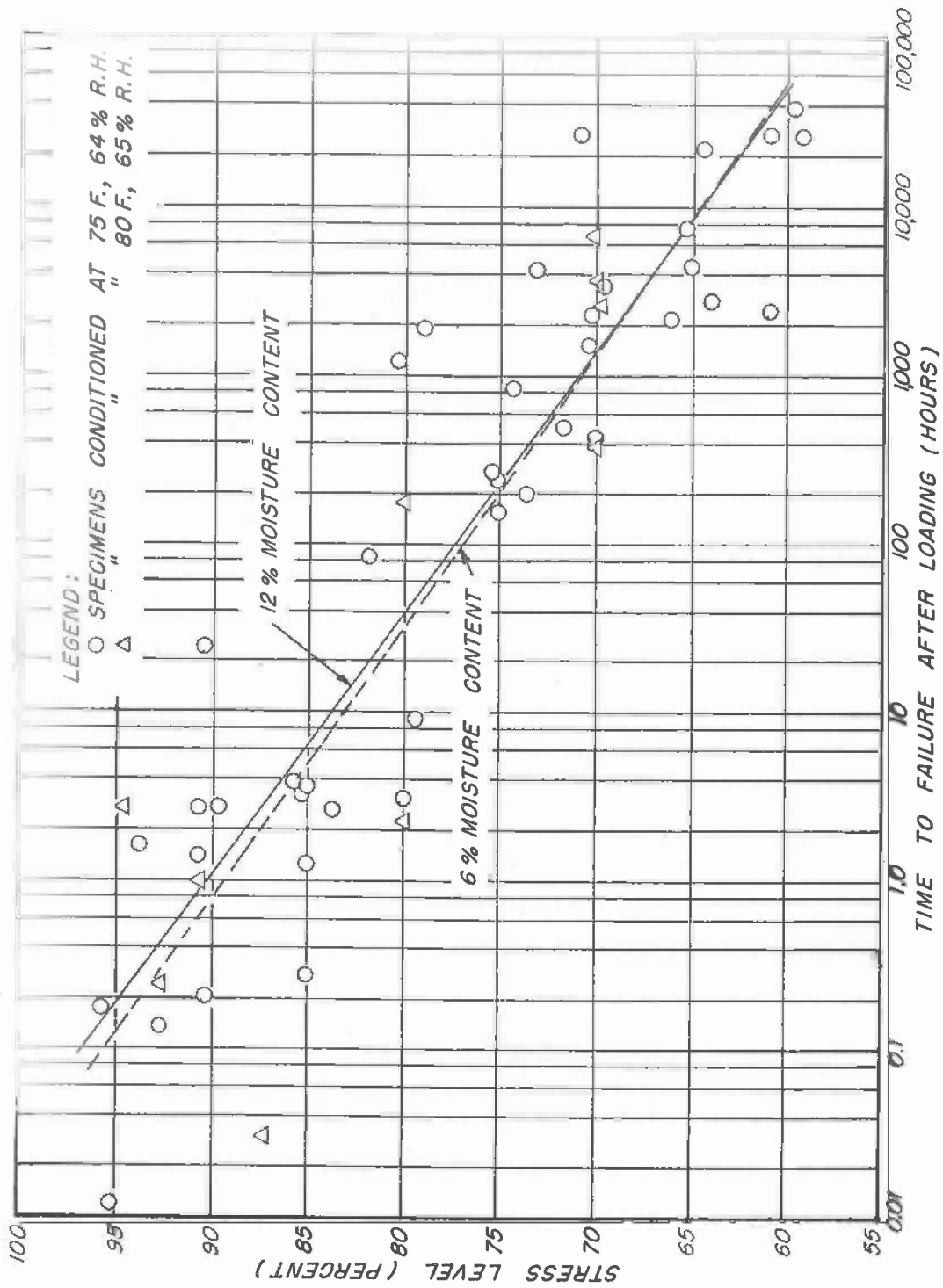


Figure 19. --Relationship between stress level and time to failure after loading at 12 percent moisture content.